

3. Electronic Systems in $d = 1$

3.1 Introduction

In this chapter we undertake the general description of electrons in one dimension. There exist systems which are actually one-dimensional, as is the case of polyacetylene[1], and others which may be considered “quasi-one-dimensional”, i. e. that show conduction properties in a preferred direction. This is the case of the well-known organic charge-transfer compounds[2]. The study of electronic properties in one dimension is not, therefore, purely academic. This is also supported by the relevance of these systems in the investigation of the so-called “quantum wires” [3] and by the increasing evidence that the edge excitations in the fractional quantum Hall effect are effectively that of a one-dimensional liquid[4].

When considering a physical problem of electrons in one dimension, one may either place the emphasis on the electron-phonon interaction or turn to consider as most relevant the electron-electron interaction. Following the scope of these notes we are going to focus our interest in the latter. Even in this perspective, one may adopt two different approaches depending on the problem. One of them is well-suited to problems where there are strong correlations among electrons and localization effects are important. These use to be properties of non-conducting systems, in which the physics is supposed to be well-described by the Hubbard model[5]. The other approach is appropriate to situations in which the interactions are not so strong, leading in general to metallic behavior. This is the point of view that we are going to adopt in what follows. It will allow us to consider perturbation theory as the starting point to investigate our systems and to make the map of the space of all the couplings constants. The main achievement of this approach is to show that, opposite to what happens in three spatial dimensions, the generic behavior in one dimension is not given by the Landau Fermi liquid picture, but by the so-called Luttinger liquid. This can be already understood from the breakdown of perturbation theory, which is spoiled by infrared divergences in one spatial dimension.

In the present chapter we undertake the analysis of perturbation theory and its failure in one dimension, which we fix with the machinery of the renormalization group. Chapter 4 is devoted to introduce the general techniques of bosonization for one-dimensional fermion systems and to develop the physical

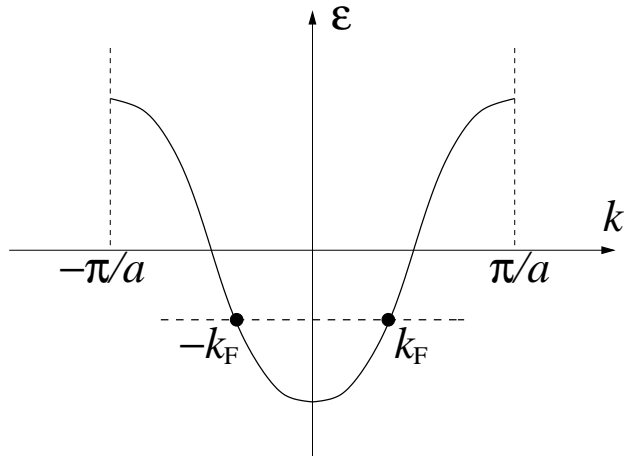


Fig. 3.1. Dispersion relation of electrons in a one-dimensional lattice.

picture of the Luttinger liquid. Finally, in Chap. 5 we discuss the correspondence of discrete models to the continuum field theory framework.

3.2 Perturbation Theory. Renormalization Group

Our one-dimensional systems have in general some kind of lattice support, given by the periodic disposition of atoms in a crystal. In tight-binding approximation, for instance, and considering only one conduction band, the electronic dispersion relation for Bloch states is given by

$$\varepsilon(k) = -t \cos ak \quad (3.1)$$

where a is the lattice spacing.

The one-particle hamiltonian in terms of the creation and annihilation operators $c_{k\sigma}^+, c_{k\sigma}$ of Bloch states is

$$H_0 = \sum_{k,\sigma} \varepsilon(k) c_{k\sigma}^+ c_{k\sigma} \quad (3.2)$$

The symbol σ denotes spin, \uparrow or \downarrow , and the label k is restricted to the first Brillouin zone $(-\pi/a, \pi/a)$. The bandwidth W is in general proportional to the hopping parameter t .

We will suppose that the Fermi level ε_F is placed somewhere in the middle of the band, not very close to its top nor to its bottom —we will see later that the effective strength of the interaction is inversely proportional to the slope at the Fermi momentum. The main feature of the electronic system in $d = 1$ is the existence of two Fermi points at $\pm k_F$, given by $\varepsilon(\pm k_F) = \varepsilon_F$. This makes possible to encode the physics of the low-energy excitations into a simple field theory, what is not feasible in general at higher dimensions. Let us consider,

for instance, processes which involve an energy $\sim E_0$ much smaller than the bandwidth W . Then it is justified to focus on the states in an interval $(-E_0, E_0)$ about the Fermi level. The dispersion relation may be linearized within this range, so that

$$\varepsilon(k) = \varepsilon_F + v_F(k - k_F) + \dots \quad \text{at the right Fermi point} \quad (3.3)$$

$$\varepsilon(k) = \varepsilon_F + v_F(-k - k_F) + \dots \quad \text{at the left Fermi point} \quad (3.4)$$

where

$$v_F = \frac{d\varepsilon}{dk}(k_F) \quad (3.5)$$

Higher orders in the expansion may be considered irrelevant, in the sense pointed out in the preceding chapter. This linear approximation, that we will use henceforth, is good in general if the interaction is not too strong and not long-ranged. The Coulomb interaction, for instance, may give rise to different effects than those considered here.

At this point we may distinguish between states attached to the right Fermi point, denoted by $a_{k\sigma}, a_{k\sigma}^+$, and states attached to the left Fermi point, denoted by $b_{k\sigma}, b_{k\sigma}^+$. In the linear approximation we may write our one-particle hamiltonian in the form

$$H_0 = \sum_{k,\sigma} v_F(k - k_F) a_{k\sigma}^+ a_{k\sigma} + \sum_{k,\sigma} v_F(-k - k_F) b_{k\sigma}^+ b_{k\sigma} \quad (3.6)$$

where we understand now that the cutoff $|\varepsilon(k) - \varepsilon_F| < E_0$ is implicit in the sum over modes.

3.2.1 Interactions

We apply now the scaling arguments introduced in the previous chapter to determine the form of the relevant or marginal interactions of the electronic system in $d = 1$. The expression (3.6) is nothing but the Dirac hamiltonian in $1 + 1$ dimensions with nonvanishing chemical potential. In terms of respective fermion fields of left and right chirality

$$\Psi_{1\sigma}(x) = \frac{1}{\sqrt{L}} \sum_k e^{ikx} b_{k\sigma} \quad (3.7)$$

$$\Psi_{2\sigma}(x) = \frac{1}{\sqrt{L}} \sum_k e^{ikx} a_{k\sigma} \quad (3.8)$$

we may write, apart from the chemical potential term,

$$H_0 = -iv_F \int dx \sum_{\sigma,j} (-1)^j \Psi_{j\sigma}^+ \partial_x \Psi_{j\sigma} \quad (3.9)$$

From this “free” hamiltonian we may read the scaling dimension of the fermion fields (in energy units) $[\Psi_j(x)] = 1/2$. We may now ask what kind of interaction

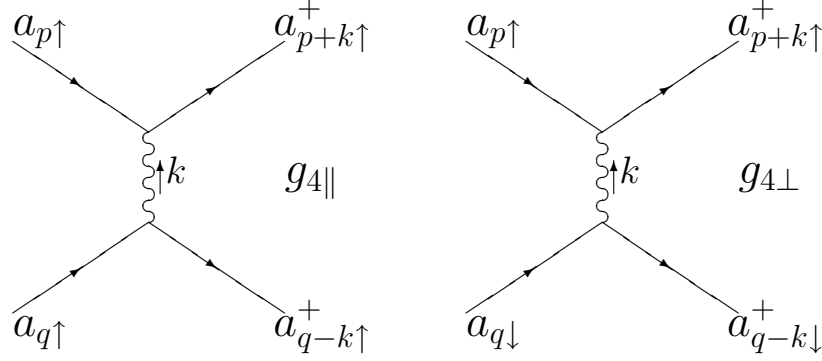


Fig. 3.2. Interactions between currents of like chirality.

hamiltonians can be built out of Ψ_1 and Ψ_2 if only dimensionless coupling constants are allowed. This catalog may still be too long, so that here we restrict it to interactions of density-times-density type. This amounts to the requirement of charge conservation in the processes under consideration. Then the only possible form of the interaction is (leaving aside subindices)

$$H_{int} \sim \int dx_1 dx_2 \Psi^+(x_1)\Psi(x_1)V(x_1, x_2)\Psi^+(x_2)\Psi(x_2) \quad (3.10)$$

where the potential $V(x_1, x_2)$ must have dimensions of energy. Obviously, terms with higher content of fermion fields have to be irrelevant, in the sense of the previous chapter, since they have to enter through coupling constants with the dimensions of positive powers of some microscopic length scale.

The collection of all the interactions of the above type is most easily summarized by drawing the corresponding Feynman diagrams in momentum space. In these we represent right modes by a full line and left modes by a dashed line. A wavy line represents the exchange of momentum through the interaction potential. Its Fourier transform introduces some structure, that we suppose to be given by some smooth function of momentum, nonsingular at $k = 0$. There are, in general, four different kinds of four-fermion interactions, according to the type of incoming and outgoing modes[6]. We consider first the interaction between two densities of the same type of modes, corresponding to diagrams with two incoming right modes and two outgoing right modes, or the same construction with right replaced by left. Even then there are two different possibilities, as shown in Fig. 3.2, depending on whether the two densities have the same or opposite spin. The coupling constant in each case is conventionally denoted by $g_{4\parallel}$ and $g_{4\perp}$.

Another different situation is when the density of left modes interacts with the density of right modes. This is illustrated in Fig. 3.3. Again the two densities may bear the same or different spin, making necessary to introduce respective coupling constants $g_{2\parallel}$ and $g_{2\perp}$.

Further on, a more ingenious interaction arises when two modes at different sides of the Fermi sea are excited to the respective opposite branches. As shown

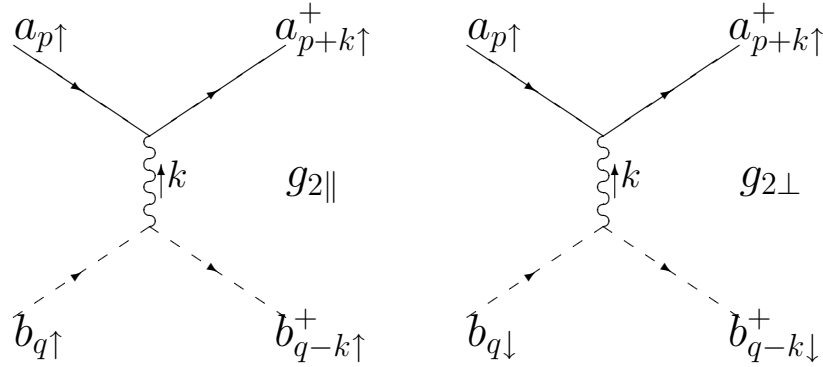


Fig. 3.3. Interactions between currents of different chirality.

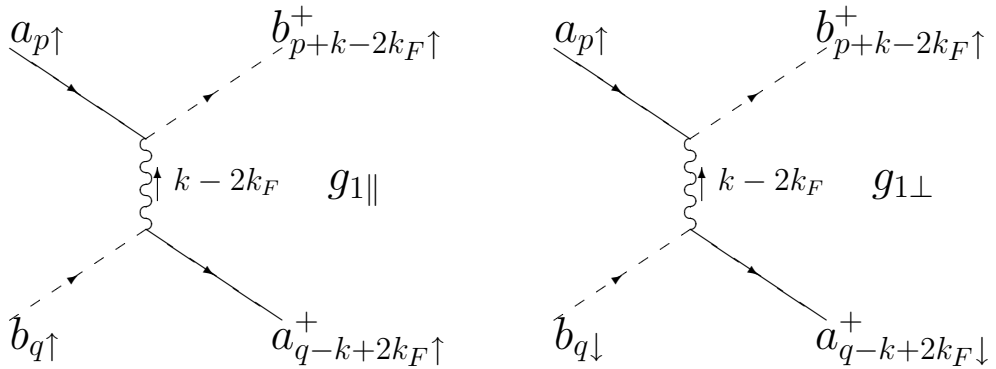


Fig. 3.4. Types of interaction with backscattering.

in Fig. 3.4, the typical momentum exchange has to be about $2k_F$. The coupling constant for this kind of interaction is now called $g_{1\parallel}$ or $g_{1\perp}$, for parallel or opposite spins at the two sides of the interaction, respectively. As we will see later, this process of backscattering introduces the main complication in the investigation of one-dimensional electron systems, as it spoils in general the integrability of the theory. The same can be said of the remaining interaction, which goes with the coupling constant g_3 and is built out of Umklapp processes. These are shown in Fig. 3.5, where the excess of momentum $4k_F$ is supposed to be absorbed by the lattice substrate. This interaction becomes relevant only at the point of half-filling, as we will see in the study of the harmonic chain in Chap. 5.

As we have already remarked, the momentum structure of the interaction is given by the Fourier transform of the potential. We have assumed that this has to be a nonsingular, smooth function for any value of k . In the rest of this chapter and for the sake of a clear exposition we will take it as a constant function of the momentum. Anyhow, our conclusions will not depend on this particular choice. In practice, it amounts to contract the interaction to a point in real space. Then, it is clear that $g_{1\parallel}$ and $g_{2\parallel}$ are describing, apart from a difference

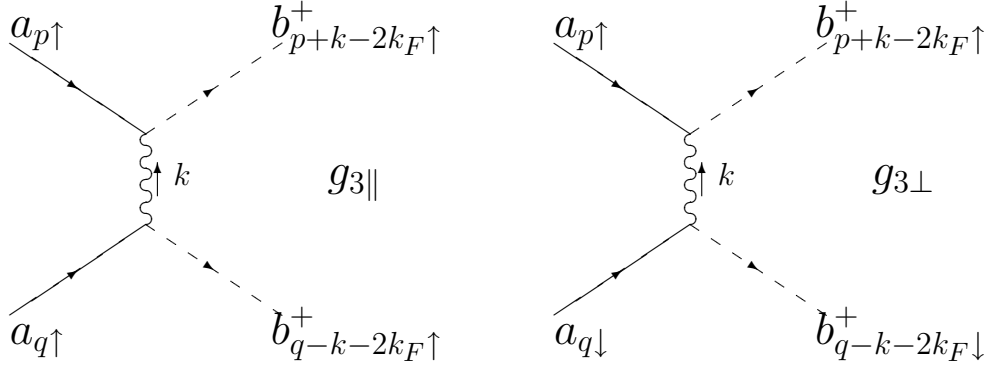


Fig. 3.5. Interactions originating from Umklapp processes.

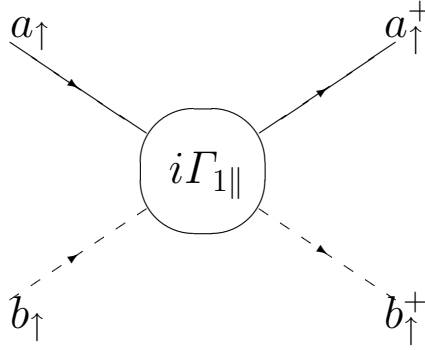


Fig. 3.6. Example of four-point vertex function.

of sign, the same kind of process. We will fix this ambiguity by making the choice $g_{2\parallel} = g_{2\perp} \equiv g_2$, so that only three independent couplings, $g_{1\parallel}$, $g_{1\perp}$ and g_2 , remain[6]. We will use this convention to the end of this chapter.

3.2.2 Quantum Corrections

Now that we have written down the possible interaction terms in the hamiltonian, we want to investigate some of the properties of the quantum theory. We follow here the philosophy adopted in quantum field theory, in that the interaction corrects the “bare” coupling constants and promotes them to respective vertex functions. One of these, that we call $\Gamma_{1\parallel}$, is represented in Fig. 3.6, where the circle stands for all possible interactions connecting the external legs. The object can be computed in perturbation theory, the zeroth order being obviously the value of $g_{1\parallel}$ according to our above redefinition.

We undertake the computation of the first order corrections in $\Gamma_{1\parallel}$, from which one gains insight of the problems to define such object. Resorting to Feynman diagrams, there are essentially three different contributions, represented in Fig. 3.7. In diagram (a) the two interactions have to be $g_{1\parallel}$, and in diagram (b) they both can be either $g_{1\parallel}$ or $g_{1\perp}$. It can be checked that, opposite

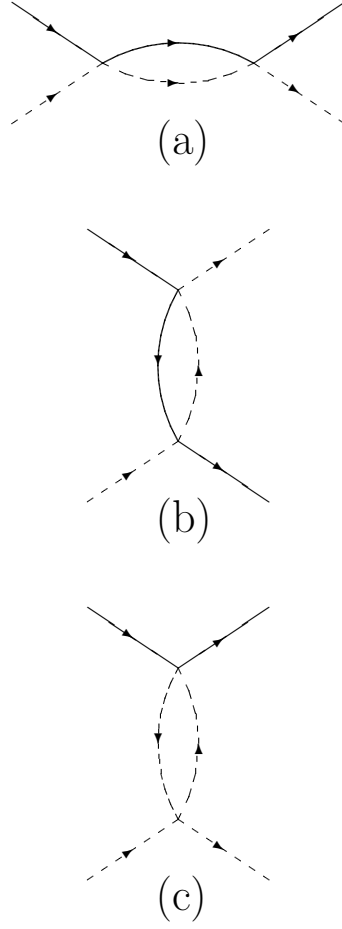


Fig. 3.7. Diagrams contributing to $\Gamma_{1\parallel}$ to the one-loop order.

to what happens with these two diagrams, the contribution of diagram (c) does not give rise to logarithmic divergences, so that it can be neglected in what follows.

The particular kinematics that we take for diagram (a) is indicated in Fig. 3.8 . The internal propagators for right modes and left modes are, respectively,

$$G_R^{(0)}(\omega, k) = \frac{1}{\omega - v_F(k - k_F) + i\epsilon \operatorname{sgn}(k - k_F)} \quad (3.11)$$

$$G_L^{(0)}(\omega, k) = \frac{1}{\omega - v_F(-k - k_F) + i\epsilon \operatorname{sgn}(-k - k_F)} \quad (3.12)$$

The contribution to $\Gamma_{1\parallel}$ from diagram (a) is therefore

$$\begin{aligned} \Gamma_{1\parallel}^{(a)} &= \\ &= -i2g_{1\parallel}^2 \int \frac{dk}{2\pi} \frac{d\omega}{2\pi} G_R^{(0)}(\omega_1 + \omega, k_F + k) G_L^{(0)}(\omega_2 - \omega, -k_F - k) \\ &= -i2g_{1\parallel}^2 \int \frac{dk}{2\pi} \frac{d\omega}{2\pi} \frac{1}{\omega_1 + \omega - v_F k + i\epsilon \operatorname{sgn}(k)} \frac{1}{\omega_2 - \omega - v_F k + i\epsilon \operatorname{sgn}(k)} \end{aligned}$$

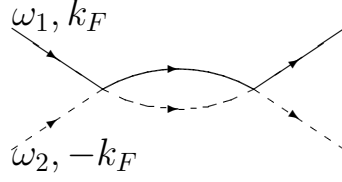


Fig. 3.8. Diagram (a) of the previous figure, with the kinematics used in its computation.

$$= i2g_{1\parallel}^2 \int \frac{dk d\omega}{2\pi 2\pi} \frac{1}{\bar{\omega} + \omega - v_F k + i\epsilon \operatorname{sgn}(k)} \frac{1}{\omega + v_F k - i\epsilon \operatorname{sgn}(k)} \quad (3.13)$$

where we have called $\omega_1 + \omega_2 \equiv \bar{\omega}$. We can perform first the k integral by working in the complex k plane. If we take $\omega > 0$ (we suppose that $\bar{\omega} > 0$), we find a pole slightly over the real axis at $(\bar{\omega} + \omega)/v_F$ and another slightly under the real axis at $-\omega/v_F$. The result of the integral is, for $\omega > 0$,

$$\begin{aligned} -i2g_{1\parallel}^2 \int_{\omega>0} \frac{d\omega}{2\pi} \frac{2\pi i}{2\pi} \frac{1}{v_F} \frac{1}{\bar{\omega} + 2\omega} &= 2g_{1\parallel}^2 \frac{1}{2\pi v_F} \int_0^{E_0} d\omega \frac{1}{\bar{\omega} + 2\omega} \\ &\approx -g_{1\parallel}^2 \frac{1}{2\pi v_F} \log \frac{\omega_1 + \omega_2}{E_0} \end{aligned} \quad (3.14)$$

where we have made use of the bandwidth cutoff E_0 . It can be checked that the contribution for $\omega < 0$ gives the same result. The total contribution from this diagram is therefore

$$\Gamma_{1\parallel}^{(a)} = -g_{1\parallel}^2 \frac{1}{\pi v_F} \log \frac{\omega_1 + \omega_2}{E_0} \quad (3.15)$$

We turn now to the contribution of diagram (b). We evaluate it in the particular kinematics shown in Fig. 3.9 (in the case $\omega_1 - \omega_3 > 0$). Following the same steps as before we get

$$\begin{aligned} \Gamma_{1\parallel}^{(b)} &= \\ &= -i2(g_{1\parallel}^2 + g_{1\perp}^2) \int \frac{dk d\omega}{2\pi 2\pi} G_R^{(0)}(\omega, k_F + k) G_L^{(0)}(\omega_3 - \omega_1 + \omega, -k_F + k) \\ &\approx (g_{1\parallel}^2 + g_{1\perp}^2) \frac{1}{\pi v_F} \log \frac{\omega_1 - \omega_3}{E_0} \end{aligned} \quad (3.16)$$

Finally, by adding up the contributions from diagrams (a) and (b) we get the result for the vertex function to first order in perturbation theory

$$\Gamma_{1\parallel} = g_{1\parallel} - g_{1\parallel}^2 \frac{1}{\pi v_F} \log \frac{\omega_1 + \omega_2}{E_0} + (g_{1\parallel}^2 + g_{1\perp}^2) \frac{1}{\pi v_F} \log \frac{\omega_1 - \omega_3}{E_0} + \dots \quad (3.17)$$

There are two important observations to be made about this expression. The first of them is that, apparently, the value of $\Gamma_{1\parallel}$ depends on the particular value chosen for the cutoff E_0 . This is actually inadmissible, since we may think of the

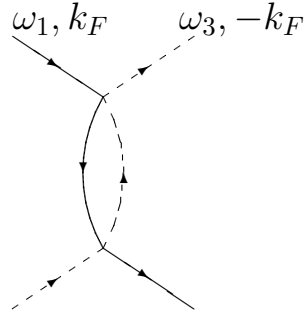


Fig. 3.9. Diagram (b) of Fig. 3.7, with the kinematics used in its computation.

vertex function as the “body” which allows us to obtain a four-point scattering amplitude just by inserting the appropriate modes in place of the external legs. This latter object is directly observable, and cannot depend on the cutoff as far as we are dealing with a predictive theory. The second remark concerns the divergence of (3.17) at small frequency values. This again cannot be a sensible effect, especially when this singularity appears even more pronounced at higher levels in perturbation theory. It can be checked, for instance, that the iteration of diagram (a) giving an n -loop contribution to the vertex function behaves like $\sim \log^n(\omega/E_0)$. Therefore what we are really observing is the breakdown of standard perturbation theory. We are going to see, however, how the first shortcoming is related, in a certain sense, to the second, and leads to the key idea giving physical meaning to the vertex function through the machinery of the renormalization group.

3.2.3 Renormalization Group

We have already learned in Chap. 2 how the ideas underlying the renormalization group can be applied to quantum statistical problems in which some energy scale can be varied by orders of magnitude. We face here one of these situations, since our aim is to make physical sense of a theory with a built-in cutoff E_0 . This may start being of the same order than the bandwidth W but much smaller than the typical energy of the electron interactions. Opposite to the approach to renormalization group based on a statistical physics description, we are going to place the emphasis on the philosophy usually adopted in quantum field theory. According to this point of view, our pretension will be to absorb the dependencies on the cutoff by applying some renormalization program. The outcome of this implementation is that the renormalization group is doing for us the partial sum of perturbation theory, in such a way that the above mentioned logarithmic divergences are cured. Actually, the problem of perturbation theory of electrons in one dimension is only one example of a recurrent logarithmic problem which appears in many different contexts, like the X-ray edge singularity problem, the Kondo effect, etc. In all these cases the recipe is to perform a partial sum of

the perturbative expansion to get rid of the logarithms and obtain the right frequency (or energy) dependence.

Let us state the basic idea behind the renormalization group[7]. In a quantum (many-body) theory where there is an available energy scale, a change of the scale in posing a given problem leads to an effective hamiltonian description with different couplings at the new scale. Applied to our particular expression (3.17), this means that we may want perhaps to change the scale of energy E_0 , but cannot then pretend to keep constant all the couplings. We have to allow for modifications of the “coupling constants” with E_0 , so that a quantity like $\Gamma_{1\parallel}$ which may be used to compute an observable remains cutoff independent. The requirement of renormalizability is actually very strong for a quantum field theory. It means that all the dependence on the cutoff of physical quantities can be absorbed by redefinitions of the couplings and the scale of the fields[8]. To the extent in that it has been studied, our quantum theory of electrons with the given set of couplings has proven to be renormalizable, which gives us the right to adopt the quantum field theory point of view.

We illustrate the property of renormalizability in a very simple instance. In general we impose a relation of the couplings and the fields to renormalized partners which do not depend on the cutoff

$$g(E_0) = Z_g(E_0)g_R \quad (3.18)$$

$$\Psi(E_0) = Z_\Psi(E_0)\Psi_R \quad (3.19)$$

Usually, the knowledge that one has of Z_g and Z_Ψ is only perturbative. Working to the first order and collecting all the dependencies on E_0 we obtain the condition for the cutoff independence of the vertex function (3.17)

$$\frac{d}{dE_0} \left\{ g_{1\parallel}(E_0) - g_{1\perp}^2(E_0) \frac{1}{\pi v_F} \log E_0 + \dots \right\} = 0 \quad (3.20)$$

In order to get a simple expression let us address the case of spin-independent interactions, that is $g_{1\parallel} = g_{1\perp}$. We obtain then

$$E_0 \frac{d}{dE_0} g_1(E_0) = \frac{1}{\pi v_F} g_1^2(E_0) + \text{higher orders} \quad (3.21)$$

This equation encodes at this level all the information from the renormalization group, since it tells us how do we have to change the coupling constant by a modification of the cutoff, in order to maintain invariant the vertex function. Now suppose that we do not want to describe a given problem at the scale E_0 but want to consider another scale E , which in general may be different by several orders of magnitude. The relation between the coupling constants at the two different scales is given by the integral of (3.21)

$$-\frac{1}{g_1(E)} + \frac{1}{g_1(E_0)} = \frac{1}{\pi v_F} \log \frac{E}{E_0} \quad (3.22)$$

or, finally,

$$g_1(E) = \frac{g_1(E_0)}{1 - (g_1(E_0)/\pi v_F) \log(E/E_0)} \quad (3.23)$$

Equation (3.23) displays the full insight of the renormalization group. We learn from it that, if we started at a scale E_0 with a coupling $g_1 > 0$ and turned to pose the problem at a smaller scale E , the effective coupling constant becomes reduced. Thus, if the original g_1 was already small (compared to πv_F) the predictions that we get from (3.23) have to be increasingly good. On the other hand, if we had started with a coupling $g_1 < 0$, by progressing to lower scales $E \ll E_0$, we would reach a point in which the effective coupling blows up. Well before this, however, our perturbative renormalization group approach must have lost its applicability. This accelerated growth of the coupling constant points at the onset of some instability which is beyond the framework of perturbation theory. We will comment ahead on the nature of the ground state in the repulsive ($g_1 > 0$) regime.

The main application of the renormalization group arises by trading the notion of the variable scale of energy E by the typical frequency at which a process is measured. If we interpret $g_1(E)$ as the effective value of the vertex function we get

$$\Gamma_1(\omega) \approx \frac{g_1(E_0)}{1 - (g_1(E_0)/\pi v_F) \log(\omega/E_0)} \quad (3.24)$$

This is the solution to the logarithmic problem posed by perturbation theory. Actually, it is known since long ago that the expression (3.24) arises also from the sum of certain class of diagrams in perturbation theory[9]. These are the so-called “parquet diagrams”, which are obtained by repeated insertion of diagrams (a) and (b) of Fig. 3.7 into themselves. The above form of the vertex function has also the virtue of being independent of the value of the cutoff E_0 —the remaining problem we wanted to fix. This is not strange, since it is the starting point of the renormalization group. If a change of the cutoff is made to E'_0 taking care of changing also the value of g_1 , it can be checked that the value of Γ_1 in (3.24) remains invariant. From this expression we arrive again at the conclusion that, even in the neighborhood of vanishing coupling constant, the physics of the attractive interaction ($g_1 < 0$) is quite different to that of repulsive interaction ($g_1 > 0$), as we see that only in the latter case makes sense the notion of small perturbation.

The most interesting analysis, however, is that of the space of couplings with $g_{1\parallel} \neq g_{1\perp}$. In this case one has to solve a coupled set of differential renormalization group equations (one for each coupling constant). The form of the integrals as the value of the cutoff is decreased gives the flow of the renormalization group in coupling constant space. The most important issue is to determine the regions in which the flow is stable (bounded) and the regions in which it is not. The most illustrative flow diagram appears in the $(g_{1\perp}, g_{1\parallel})$ plane. It is represented in Fig. 3.10, as the result of solving the first order renormalization group equations.

This is a rather familiar phase diagram in condensed matter physics, since it appears also in quite different instances as the anisotropic Kondo problem[10]

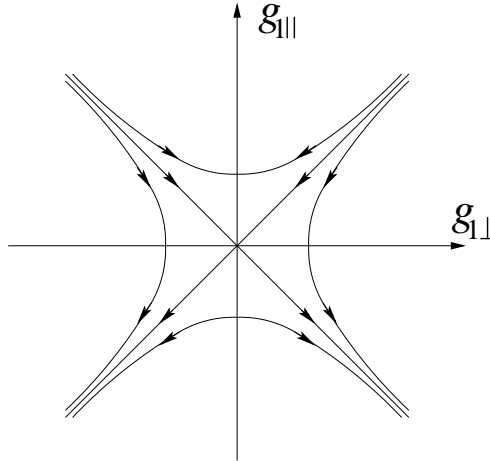


Fig. 3.10. Renormalization group flow in $(g_{1\perp}, g_{1\parallel})$ space.

or the Kosterlitz-Thouless phase transition[11]. We see that in the region $g_{1\parallel} \geq |g_{1\perp}|$ the flow is stable and leads always to a fixed point over the $g_{1\perp} = 0$ line. We remind that the meaning of the flow is that a problem with a certain set of coupling constants at a given scale is equivalent to another with lower energy scale and coupling constants found ahead in the corresponding orbit of the flow. This implies that a system in the region $g_{1\parallel} \geq |g_{1\perp}|$ must have physical properties related to another in which the backscattering mediated by $g_{1\perp}$ can be neglected. This is of great help, as we will see in the next chapter, since the model with $g_{1\perp} = 0$ is a gapless, integrable system. On the other hand, in the region $g_{1\parallel} < |g_{1\perp}|$ the flow is not bounded at this level, and the physical properties cannot be easily predicted. There is a horizontal line of points in the lower half-plane (Luther-Emery line) in which the theory can be solved, though this is not a line of fixed points[6]. There is evidence that in this regime the system ends up acquiring a gap in the spin excitation spectrum, which is the signal of an incipient superconductivity.

3.2.4 Ground State Properties

We now turn to the question of the nature of the ground state of the one-dimensional systems. This is studied by looking at the response functions, which give the hint of the kind of fluctuations which dominate at $T = 0$. In general one may expect instabilities of superconducting, charge density wave and spin density wave type. In these one-dimensional systems one cannot have true long-range order, yet it is possible to study the divergence of the response functions in ω at certain values of the momentum and determine in this competition which fluctuation prevails at low energy.

The response function related to a given charge, spin or superconductivity pairing operator \mathcal{O} is defined by

$$R(\omega, k) = -i \int dt e^{i\omega t} \langle \mathcal{O}(t, k) \mathcal{O}^+(0, k) \rangle \quad (3.25)$$

In the case of the charge or the spin density operator, $R(\omega, k)$ follows at $k = 2k_F$ a power law behavior ω^α for small ω , which gives the measure of the instabilities present in the system[6]. One is led therefore to study the dynamic correlations for the charge density operator

$$\mathcal{O}_{CDW}(t, k + 2k_F) = \sum_p a_{p+k+2k_F\uparrow}^+ b_{p\uparrow} + \sum_p a_{p+k+2k_F\downarrow}^+ b_{p\downarrow} \quad (3.26)$$

the spin density operator

$$\mathcal{O}_{SDW}(t, k + 2k_F) = \sum_p a_{p+k+2k_F\uparrow}^+ b_{p\uparrow} - \sum_p a_{p+k+2k_F\downarrow}^+ b_{p\downarrow} \quad (3.27)$$

the singlet pairing operator

$$\mathcal{O}_{SP}(t, k) = \sum_p a_{p+k\uparrow} b_{-p\downarrow} + \sum_p b_{-p\uparrow} a_{p+k\downarrow} \quad (3.28)$$

and the triplet pairing operator

$$\mathcal{O}_{TP}(t, k) = \sum_p a_{p+k\uparrow} b_{-p\downarrow} - \sum_p b_{-p\uparrow} a_{p+k\downarrow} \quad (3.29)$$

The power law behavior ω^α of the response functions is consistent with the fact that under the renormalization group the correlators get anomalous dimensions at small ω . To see how this works, let us consider the correlation of the charge density operator, in the simple case of spin-independent interactions $g_{1\parallel} = g_{1\perp}$. In the noninteracting theory, the corresponding response function $R_{CDW}(\omega, k)$ is given by a single particle-hole loop of the same type that appears in Fig. 3.9 . We already know the result for this object from (3.16). To zeroth order in perturbation theory we have

$$R_{CDW}(\omega, 2k_F) = \frac{1}{\pi v_F} \log \frac{\omega}{E_0} + O(g^2) \quad (3.30)$$

where ω is now the external frequency injected into the loop. The first perturbative corrections appear by iterating the loop by means of g_1 interactions or by inserting a g_2 interaction in the middle of it. Adding up both contributions we have

$$R_{CDW}(\omega, 2k_F) = \frac{1}{\pi v_F} \log \frac{\omega}{E_0} \left(1 + \frac{2g_1 - g_2}{2\pi v_F} \log \frac{\omega}{E_0} + \dots \right) \quad (3.31)$$

We observe that the iteration of the above operations in the loop produces more severe logarithmic divergences to higher orders in the interaction. This is an indication that the breakdown of perturbation theory arises from the wrong expansion of an exponential dependence on the coupling constants. Renormalization group methods allow to reproduce again the correct dependence by exploiting the scaling properties of the correlator with respect to changes in the

cutoff E_0 . If we take the derivative of $R_{CDW}(\omega, 2k_F)$ with respect to E_0 , we have to bear in mind the explicit dependences at the right-hand-side of (3.31) as well as the implicit dependences of the coupling constants on the cutoff. However, if we apply the derivative on g_1 or g_2 , this produces higher order terms according to (3.21). Therefore, to first order we have

$$\frac{\partial}{\partial E_0} R_{CDW} = -\frac{1}{\pi v_F} \frac{1}{E_0} \left(1 + \frac{2g_1 - g_2}{\pi v_F} \log \frac{\omega}{E_0} + \dots \right) \quad (3.32)$$

Within the same approach of the perturbative renormalization group, we may replace $(\pi v_F)^{-1} \log(\omega/E_0)$ in the second term of the derivative by the full response function R_{CDW} , the difference being of higher order in the coupling constants. Finally we get the differential equation

$$\frac{\partial}{\partial E_0} R_{CDW} = -\frac{1}{\pi v_F} \frac{1}{E_0} (1 + (2g_1 - g_2)R_{CDW} + \dots) \quad (3.33)$$

In order to obtain the dominant behavior of R_{CDW} , we observe that $g_1(E_0)$ and $g_2(E_0)$ are both regular at small values of the cutoff (for $g_1 > 0$). The only singularities may arise due to the $1/E_0$ factor at the right-hand-side of (3.33) and g_1 and g_2 can be set to their respective fixed-point values, 0 and g_2^* . The solution of (3.33) has therefore the leading behavior

$$R_{CDW} \sim \left(\frac{\omega}{E_0} \right)^{\alpha_{CDW}} \quad (3.34)$$

with $\alpha_{CDW} = -g_2^*/(\pi v_F)$. We remark that the combination $g_2 - g_1/2$ is a renormalization group invariant, to the order we are working here. Therefore, in terms of the original couplings we have $\alpha_{CDW} = -(g_2 - g_1/2)/(\pi v_F)$. By means of similar calculations, one may check that the rest of exponents for the spin density, singlet pairing and triplet pairing response functions are given respectively by

$$\alpha_{SDW} = -(g_2 - g_1/2)/(\pi v_F) \quad (3.35)$$

$$\alpha_{SP} = (g_2 - g_1/2)/(\pi v_F) \quad (3.36)$$

$$\alpha_{TP} = (g_2 - g_1/2)/(\pi v_F) \quad (3.37)$$

Characterizing the nature of the ground state by the most singular behavior among the mentioned response functions, one may draw the phase diagram in the coupling constant space. This is shown in Fig. 3.11 for the region $g_1 > 0$, which is susceptible of perturbative treatment. For $g_2 > g_1/2$ we may expect a tendency to the formation of a charge density wave or a spin density wave in the ground state of the theory. On the contrary, for $g_2 < g_1/2$ the superconductivity pairing correlations are supposed to dominate the system. Though we have only worried about the power-law dependence of the response functions, these are affected by logarithmic corrections, which enhance the spin density or the triplet pairing instability over the charge density or the singlet pairing instability in the corresponding situation.

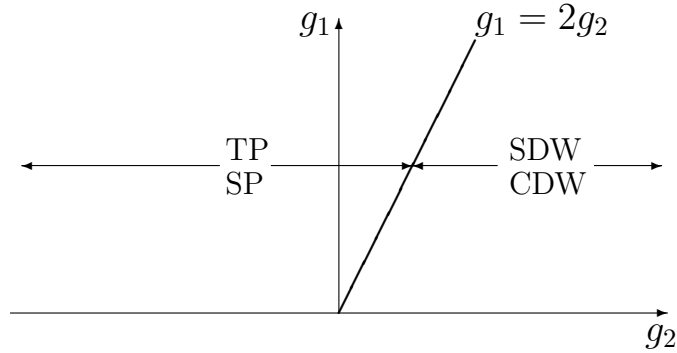


Fig. 3.11. Phase diagram of the one-dimensional electron system with spin-independent interactions.

We may think of the power-law dependence of the response functions as a reflection of the critical behavior of the system, though the exponents that we find are non-universal, i.e. they depend on the coupling constants of the model. On the other hand, the correlations are enhanced with respect to those of the noninteracting theory. The logarithmic behavior in (3.30) translates into a power-law decay in real space (t, x) of the form $\sim 1/x^2$, while a scaling of the type (3.34) gives rise to a long-distance behavior $\sim 1/x^{2+\alpha}$. For the corresponding response function with $\alpha < 0$, this slower decay reflects a tendency to order, which cannot be attained anyhow as far as in two space-time dimensions a continuous symmetry cannot be spontaneously broken. We will find again the phenomenon of enhancement at $2k_F$ when discussing the correlation functions of the Hubbard model in Chap. 5.

We close this chapter by remarking that the above physical picture has to be taken with the reserve inherent to a perturbative treatment. In particular, it is not guaranteed that modifications of the flow and new physics may not arise for sufficiently large values of the couplings. In the unstable phase $g_1 < 0$ we even lack a perturbative description of the low-energy physics. What would be needed is actually some specific modelling of the large attractive interaction. These and other questions, as the effects of band curvature, are still open problems in the topic of one-dimensional electron systems.

exercise 3.1 Compute the contribution to $\Gamma_{1\parallel}$ from the diagram in Fig. 3.9 .

exercise 3.2 Check that the value of $\Gamma_1(\omega)$ in (3.24) is invariant under the change to a different cutoff E'_0

References

- [1]A. J. Heeger, S. Kivelson, J. R. Schrieffer and W. P. Su, *Rev. Mod. Phys.* **60** (1988) 781.
- [2]D. Jérôme and H. J. Schulz, *Adv. Phys.* **31** (1982) 299. See also D. Jérôme and L. G. Caron, *Low-Dimensional Conductors and Superconductors* (Plenum, New York, 1987).
- [3]C. L. Kane and M. P. A. Fisher, *Phys. Rev. B* **46** (1992) 15233.
- [4]F. P. Milliken, C. P. Umbach and R. A. Webb, to be published in *Phys. Rev. Lett.*
- [5]J. Hubbard, *Proc. R. Soc. A* **276** (1963) 238.
- [6]J. Sólyom, *Adv. Phys.* **28** (1979) 201.
- [7]L. P. Kadanoff, *Rev. Mod. Phys.* **49** (1977) 267; K. G. Wilson, *Rev. Mod. Phys.* **55** (1983) 583.
- [8]P. Ramond, *Field Theory. A Modern Primer.* (Addison-Wesley, Reading, 1989).
- [9]Yu. A. Bychkov, L. P. Gorkov and I. E. Dzyaloshinsky, *Soviet Phys. JETP* **23** (1966) 489. In the context of the Kondo effect, see also A. A. Abrikosov, *Physics* **2** (1965) 5. Regarding the X-ray edge singularity problem, see B. Roulet, J. Gavoret and P. Nozières, *Phys. Rev.* **178** (1969) 1072.
- [10]P. W. Anderson, G. Yuval and D. R. Hamann, *Phys. Rev. B* **1** (1970) 4464.
- [11]J. M. Kosterlitz, *J. Phys. C* **7** (1974) 1046.

4. Bosonization. Luttinger Liquid

4.1 Luttinger Model. Bosonization

In this section we are going to focus our attention on the line of critical points $g_{1\perp} = 0$ in the upper half-plane of Fig. 3.10 . These are worth of study since, as stated in the previous chapter, the properties of the theory on that line give the low-energy physics on the whole region $g_{1\parallel} \geq |g_{1\perp}|$, where the backscattering is an irrelevant perturbation. The model with $g_{1\perp} = 0$ is called the Tomonaga model[1]. A further simplification is achieved if one introduces an infinite linear dispersion relation for both left and right channels, as shown in Fig. 4.1 . It is argued that the influence of the deeper, spurious electronic states can be neglected if one only cares about low-energy processes. The consequences of this variant are important since the model with the infinite linear dispersion relation and the interactions given in Figs. 3.2 and 3.3 is exactly solvable. This is called the Luttinger model[2]. Quite remarkably, this is a quantum field theory in which the complete summation of diagrams in perturbation theory can be achieved[3]. This can be done using the great degree of symmetry of the model: the dynamics conserves the number of particles of given spin in a given channel.

We will not adopt, though, the perturbative approach to solve the Luttinger model. Instead we will introduce bosonization techniques which are well-suited for more general problems in 1+1 dimensions. Haldane has made plausible that certain properties that one describes by means of bosonization are robust, in the sense that they should be shared also by the more realistic one-dimensional electron systems (whenever backscattering can be neglected). These properties configure a kind of universality class, referred to by the name of Luttinger liquid[4]. Its most prominent feature is the absence of quasiparticles with the same quantum numbers of the electron, together with the possibility of classifying all the excitations into boson-like objects. These account, in general, for charge and spin degrees of freedom, whose dynamics becomes completely independent.

4.1.1 Bosonic Excitations

We begin by classifying the excitations of the non-interacting Luttinger model. Since in the present development the two possible orientations of spin play

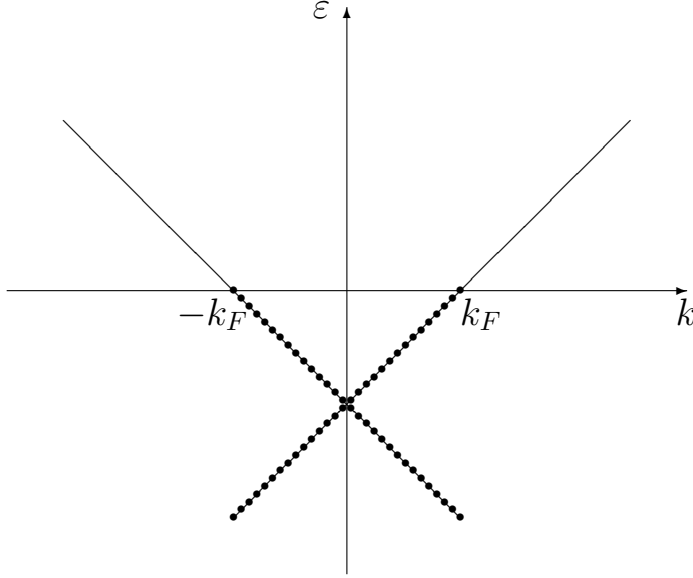


Fig. 4.1. Electronic dispersion relation in the Luttinger model.

parallel roles we will simply omit them, instead of duplicating all the expressions (spin requires an explicit consideration, however, when the interactions are turned on). Our “free” hamiltonian reads then

$$H_0 = \sum_k v_F(k - k_F) a_k^+ a_k + \sum_k v_F(-k - k_F) b_k^+ b_k \quad (4.1)$$

where, according to the infinite dispersion relation, no cutoff is implied in the sum over modes.

If we think of all the possible ways in which one can confer energy to the Fermi sea represented in Fig. 4.1, we find three essentially different operations in which this can be done.

i) Density excitations

The first may consist of taking an electron of the Fermi sea, in a given channel, and promoting it to an empty state above the Fermi level, in the same branch of the dispersion relation. In practice one considers the linear combination of operations involving the same excitation energy, for instance

$$\rho_{kR} = \sum_q a_{q+k}^+ a_q \quad (4.2)$$

for the right branch, and

$$\rho_{kL} = \sum_q b_{q+k}^+ b_q \quad (4.3)$$

for the left branch.

Now, it is clear that for $k > 0$ ρ_{kR} creates an excitation while ρ_{kL} desexcites the Fermi sea. For $k < 0$ the roles are reversed. These operators cannot be interpreted yet as true creation and annihilation operators, since their commutation relations do not have the proper normalization. It can be shown that

$$[\rho_{-k'R}, \rho_{kR}] = \delta_{kk'} k \frac{L}{2\pi} \quad (4.4)$$

$$[\rho_{-k'L}, \rho_{kL}] = -\delta_{kk'} k \frac{L}{2\pi} \quad (4.5)$$

We have supposed for convenience that the electrons are confined in a compact dimension of length L . The proof of the commutation relations (4.4), (4.5) has actually some subtle points that can be conveniently dealt with taking into account the infinite linear dispersion relation[5]. If one only cares about low-energy excitations, though, the same results can be obtained by using a linear dispersion relation with bandwidth cutoff. We give a sketch of the proof of (4.4) and (4.5) in this latter case. Suppose that we consider the region of momentum space between $-\Lambda + k_F \equiv k_1$ and $\Lambda + k_F \equiv k_2$. The commutator of ρ_{-kR} and ρ_{kR} , for instance, reads

$$\begin{aligned} [\rho_{-kR}, \rho_{kR}] &= \left[\sum_{k_1 < q-k, q < k_2} a_{q-k}^+ a_q, \sum_{k_1 < r+k, r < k_2} a_{r+k}^+ a_r \right] \\ &= \sum_{k_1 < r, r+k < k_2} \delta_{q, r+k} a_{q-k}^+ a_r \\ &\quad - \sum_{k_1 < q, q-k < k_2} \delta_{r, q-k} a_{r+k}^+ a_q \end{aligned} \quad (4.6)$$

It is important to have in mind that in these sums all the subindices run between k_1 and k_2 . For this reason, provided that $0 < k < \Lambda$, one can see that the first sum in (4.6) has k over $2\pi/L$ more contributions than the other from the lower part of the band, while the second gets the same number in excess from the upper part of the band. We may now replace the right-hand-side of (4.6) by its vacuum expectation value on the ground state, which is an increasingly good approximation as $\Lambda \rightarrow \infty$ or, equivalently, at low-energies. Since the number operator $a_r^+ a_r$ gives zero acting on states above k_F , we get $kL/(2\pi)$ for the final result of the commutator.

At this point, we form boson creation and annihilation operators by defining

$$\begin{aligned} B_k^+ &= \sqrt{\frac{2\pi}{L|k|}} \rho_{kR} \quad k > 0 \quad , \quad B_k^+ = -\sqrt{\frac{2\pi}{L|k|}} \rho_{kL} \quad k < 0 \\ B_k &= \sqrt{\frac{2\pi}{L|k|}} \rho_{-kR} \quad k > 0 \quad , \quad B_k = -\sqrt{\frac{2\pi}{L|k|}} \rho_{-kL} \quad k < 0 \end{aligned} \quad (4.7)$$

These obey the canonical commutation relations

$$[B_k, B_{k'}^+] = \delta_{kk'} \quad (4.8)$$

In this boson representation, the unexcited Fermi sea is equivalent to the boson ground state, defined as the state which is annihilated by all the B_k . The energy associated to the creation of each boson is obviously $v_F |k|$.

ii) Current excitations

We may imagine, furthermore, a second type of excitation process of the Fermi sea. It arises when a number of electrons of one of the branches are taken from below the Fermi level and shifted to the other branch. For a given number of shifted electrons, we are going to be interested in the *minimal* energy needed in the process. Thus, in the case of one electron we have to take it at the Fermi level, say from the left channel, and place it on top of the highest occupied level in the right channel. One has to remember that the system has spatial periodicity equal to L , so that the distance between neighboring states in momentum space is $2\pi/L$. The energy involved in shifting one electron is therefore this quantity times v_F .

In the process of transferring two electrons from one channel to the other, we have to realize that, after having shifted the first, the second electron is pulled from a state which is at a distance $2\pi/L$ of the Fermi level. As it has to be placed on top of the previously transferred electron, the total energy involved in the process is $2\pi/L$ times $v_F(1 + 3)$. It is not hard to see that the energy needed in the case of three electrons is $2\pi/L$ times $v_F(1 + 3 + 5)$, in the case of four electrons $2\pi/L$ times $v_F(1 + 3 + 5 + 7)$, etc. In general, the energy needed to transfer a number J of electrons can be expressed in compact form as $(2\pi/L)v_F J^2$ [4]. What is important to realize is that J is also half the difference of the number of electrons of one channel with respect to the other. In the Luttinger model the dynamics conserves the number of electrons N_R in the right channel and the number of electrons N_L in the left channel. Therefore it is really appropriate to take J as a number, since it is a *conserved charge* of the problem. The energy for the kind of process we have just described is therefore

$$\frac{\pi}{2L}v_F(N_R - N_L)^2 \quad (4.9)$$

iii) Charge excitations

Finally, we are left with only one more possibility to excite the Fermi sea of Fig. 4.1. This is the addition of net charge to the system. In other words, we have to evaluate the dependence of the energy of the system on charge variations. Since the preceding operation involved the asymmetry in the distribution of electrons in the two branches, we will suppose for convenience that the same charge is conferred to each channel. We take the Fermi level as a reference when measuring the energy balance. Thus, after addition of one electron to each channel the energy gained by the system is $(2\pi/L)$ times $2v_F$. The energy needed to modify by two units the charge per channel is $(2\pi/L)$ times $2v_F(1 + 2)$, to modify it by three $(2\pi/L)$ times $2v_F(1 + 2 + 3)$, etc. The sequence of integer numbers appears as the result of placing each new electron on top of the previous one. In general, when the total charge added to the system is N , the balance of energy becomes $(2\pi/L)v_F(N/2 + 1)N/2$. In this operation, however, the Fermi level is risen by $v_F\delta k_F = (2\pi/L)v_F N/2$. Since we are measuring the energy with

respect to this reference level we have to discount this shift. The energy gained by addition of charge becomes then[4]

$$\frac{\pi}{2L}v_F(N_R + N_L)^2 \quad (4.10)$$

where now N_R and N_L are normal ordered quantities, i.e. measured after subtraction of the charge of the Fermi sea.

4.1.2 Bosonization

The remarkable fact is that, in one dimension, the set of bosonic excitations we have just described spans the whole Hilbert space of the original fermion problem. Thus, the basis of one-particle electron states and that of boson occupation numbers are nothing but different representations for the same quantum system. The boson excitations are all independent by construction. That they also provide a complete set of states can be shown in several ways. The most sophisticated consists of computing the partition function of the grandcanonical ensemble

$$\mathcal{Z}(\beta) = \text{tr} \exp\{-\beta H_0\} \quad (4.11)$$

in both bases and checking that the result is independent of taking the trace over fermion or boson excitations[4]. Actually, the identity between the expressions one obtains in the two cases is highly nontrivial. A quicker way of showing the equivalence of the two representations manages to compare the thermal energy for the two descriptions, in the infinite volume limit $L \rightarrow \infty$ [6]. Then, the sums over modes can be replaced by integrals which are easier to evaluate. The thermal energy in the fermion representation is

$$E_F = \sum_{k>k_F} 2 \frac{\varepsilon(k) - \varepsilon_F}{e^{\beta(\varepsilon(k) - \varepsilon_F)} + 1} \approx \frac{1}{\beta^2} \frac{L}{2\pi v_F} \int_0^\infty dx \frac{2x}{e^x + 1} \quad (4.12)$$

where the factor of 2 takes into account the energy of the holes. The same quantity in the boson representation reads

$$E_B = \sum_{k>0} \frac{\varepsilon(k)}{e^{\beta\varepsilon(k)} - 1} \approx \frac{1}{\beta^2} \frac{L}{2\pi v_F} \int_0^\infty dx \frac{x}{e^x - 1} \quad (4.13)$$

It can be checked that the two integrals in (4.12) and (4.13) give the same result, which completes the proof in the limit $v_F\beta/L \ll 1$.

As a consequence of the mentioned equivalence, we may also express the hamiltonian (4.1) in terms of the bosons B_k, B_k^\dagger and the conserved charges N_L, N_R . Recalling the energy of each mode evaluated before, we have

$$\begin{aligned} H_0 &= \sum_{k \neq 0} v_F |k| B_k^\dagger B_k + \frac{\pi}{2L} v_F (N_R - N_L)^2 + \frac{\pi}{2L} v_F (N_R + N_L)^2 \\ &= \sum_{k \neq 0} v_F |k| B_k^\dagger B_k + \frac{\pi}{L} v_F N_L^2 + \frac{\pi}{L} v_F N_R^2 \end{aligned} \quad (4.14)$$

In fact, one can organize more efficiently the boson excitations into a pair of boson fields in 1+1 dimensions. As stated before, the conserved charges N_L and N_R count additional fermions to the Fermi sea and are therefore represented by the normal ordered form of the respective zero momentum boson modes. We have, for instance,

$$N_R = \sum_q a_q^+ a_q - \left\langle \sum_q a_q^+ a_q \right\rangle \quad (4.15)$$

along with a similar expression for the left charge. It is possible to arrange ρ_{kR} and N_R into a genuine chiral boson field

$$\Phi_R(x) = \frac{2\pi}{L} \left(xN_R + i \sum_{k \neq 0} \frac{e^{-ikx}}{k} \rho_{kR} \right) \quad (4.16)$$

This field has a definite chirality since, in the sum over modes, creation operators, for instance, enter only for $k > 0$. The field with the opposite chirality is given by

$$\Phi_L(x) = \frac{2\pi}{L} \left(xN_L + i \sum_{k \neq 0} \frac{e^{-ikx}}{k} \rho_{kL} \right) \quad (4.17)$$

We have obtained this chiral decomposition quite naturally, since we have started with a problem in which the two branches of the dispersion relation are completely disconnected.

In field theory one usually deals with the complete boson field

$$\begin{aligned} \Phi(x) &= \Phi_L(x) + \Phi_R(x) \\ &= \frac{2\pi}{L} x (N_L + N_R) + i \sum_{q \neq 0} \sqrt{\frac{2\pi}{L|q|}} \left(e^{-iqx} B_q^+ - e^{iqx} B_q \right) \end{aligned} \quad (4.18)$$

The decomposition into left and right parts requires the use of the momentum field operator

$$\begin{aligned} \Pi(x) &= \frac{1}{4\pi} (\partial_x \Phi_L(x) - \partial_x \Phi_R(x)) \\ &= \frac{1}{4\pi} \left(\frac{2\pi}{L} (N_L - N_R) - \sum_{q \neq 0} \sqrt{\frac{2\pi}{L|q|}} |q| \left(e^{-iqx} B_q^+ + e^{iqx} B_q \right) \right) \end{aligned} \quad (4.19)$$

which enters in the canonical commutation relation

$$[\Phi(x), \Pi(y)] = i\delta(x - y) \quad (4.20)$$

We have actually the relations

$$\Phi_L(x) = \frac{1}{2} \left(\Phi(x) + 4\pi \int^x dy \Pi(y) \right) \quad (4.21)$$

$$\Phi_R(x) = \frac{1}{2} \left(\Phi(x) - 4\pi \int^x dy \Pi(y) \right) \quad (4.22)$$

that will be needed in the next section for the boson representation of the fermion field operator. The representation of the chiral boson fields in terms of the fermions is straightforward and reads, from (4.16) and (4.17),

$$\partial_x \Phi_L(x) = \frac{2\pi}{L} \rho_L(x) \quad (4.23)$$

$$\partial_x \Phi_R(x) = \frac{2\pi}{L} \rho_R(x) \quad (4.24)$$

In terms of the boson fields the hamiltonian (4.14) can also be expressed in integral compact form. From the above expressions it can be proven that

$$\begin{aligned} H_0 &= \int_0^L dx v_F \frac{\pi}{L^2} (: \rho_L(x) \rho_L(x) : + : \rho_R(x) \rho_R(x) :) \\ &= \frac{v_F}{2} \int_0^L dx : \left(4\pi \Pi^2(x) + \frac{1}{4\pi} (\partial_x \Phi(x))^2 \right) : \end{aligned} \quad (4.25)$$

Normal ordering in the above expression is needed to deal with singularities arising from the product of fields at the same point. This representation of the hamiltonian as a quadratic form on the density fields stems from a more general property for Kac-Moody algebras (Sugawara construction), of which ours is a trivial example[7]. As we are going to see, it plays also an essential role in the integrability of the Luttinger model.

4.1.3 Interacting Theory

As mentioned before, the Luttinger model describes points of the critical line in which only the g_2 and g_4 types of interaction are present, in the notation of Figs. 3.2 and 3.3. This makes possible to express the interacting hamiltonian, as well as the “free” hamiltonian (4.25), as a form quadratic in boson creation and annihilation operators. The $g_{1\perp}$ type of interaction cannot be written in the form “density” times “density”, which explains why the backscattering term spoils in general the integrability of the model.

According to the description of Figs. 3.2 and 3.3, the interaction hamiltonian now reads

$$\begin{aligned} H_{int} &= \frac{1}{L} \sum_{q>0} g_2(q) (\rho_{qR} \rho_{-qL} + \rho_{-qR} \rho_{qL}) \\ &\quad + \frac{1}{L} \sum_{q>0} \frac{g_4(q)}{2} (\rho_{qR} \rho_{-qR} + \rho_{-qR} \rho_{qR} + \rho_{qL} \rho_{-qL} + \rho_{-qL} \rho_{qL}) \end{aligned} \quad (4.26)$$

In what follows we let g_2 and g_4 depend on the momentum transfer q . We will see that this level of generality is needed since some constraints on the “coupling constants” arise for the strict integrability of the Luttinger model.

Aside from the zero momentum modes, we write the total hamiltonian of the interacting model in terms of the boson operators (4.7)

$$\begin{aligned}
H &= H_0 + H_{int} \\
&= v_F \sum_{q \neq 0} |q| B_q^+ B_q - \sum_{q > 0} \frac{g_2}{2\pi} |q| (B_q^+ B_{-q}^+ + B_q B_{-q}) \\
&\quad + \sum_{q > 0} \frac{g_4}{4\pi} |q| (B_q^+ B_q + B_q B_q^+ + B_{-q}^+ B_{-q} + B_{-q} B_{-q}^+) \quad (4.27)
\end{aligned}$$

It is convenient to rewrite the first term in the form

$$v_F \sum_{q \neq 0} |q| B_q^+ B_q = \frac{v_F}{2} \sum_{q \neq 0} |q| (B_q^+ B_q + B_q B_q^+) - \frac{v_F}{2} \sum |q| \quad (4.28)$$

where we suppose that the last sum is conveniently cut off in the ultraviolet. It turns out that the g_4 interaction can be absorbed into a redefinition of the “free” hamiltonian

$$\begin{aligned}
H &= \frac{1}{2} \sum_{q \neq 0} \left(v_F + \frac{g_4}{2\pi} \right) |q| (B_q^+ B_q + B_q B_q^+) - \frac{v_F}{2} \sum |q| \\
&\quad - \sum_{q \neq 0} \frac{g_2}{4\pi} |q| (B_q^+ B_{-q}^+ + B_q B_{-q}) \quad (4.29)
\end{aligned}$$

We see therefore that the effect of g_2 and that of g_4 are quite different on the electronic system. The effect of g_4 is to “renormalize” the value of the Fermi velocity

$$v_F \rightarrow v_F + \frac{g_4}{2\pi} \equiv v'_F \quad (4.30)$$

while that of g_2 is more drastic since it changes the ground state.

In fact, the total hamiltonian can be diagonalized by means of a Bogoliubov transformation[8]

$$\tilde{B}_q^+ = \cosh \phi(q) B_q^+ - \sinh \phi(q) B_{-q} \quad (4.31)$$

$$\tilde{B}_{-q} = \cosh \phi(q) B_{-q} - \sinh \phi(q) B_q^+ \quad (4.32)$$

With this parametrization, the new operators \tilde{B}_q and \tilde{B}_q^+ continue satisfying canonical commutation relations. Writing the hamiltonian in terms of them and requiring the cancellation of the $\tilde{B}_q^+ \tilde{B}_{-q}^+$ and $\tilde{B}_q \tilde{B}_{-q}$ contributions, we get the condition on $\phi(q)$

$$\tanh 2\phi(q) = \frac{1}{v'_F} \frac{g_2}{2\pi} \quad (4.33)$$

The diagonal hamiltonian reads then

$$\begin{aligned}
H &= \frac{1}{2} \sum_{q \neq 0} \tilde{v}_F |q| (\tilde{B}_q^+ \tilde{B}_q + \tilde{B}_q \tilde{B}_q^+) - \frac{v_F}{2} \sum |q| \\
&= \sum_{q \neq 0} \tilde{v}_F |q| \tilde{B}_q^+ \tilde{B}_q + \frac{1}{2} \sum (\tilde{v}_F - v_F) |q| \quad (4.34)
\end{aligned}$$

where

$$\begin{aligned}
\tilde{v}_F &= v'_F \cosh 2\phi(q) - \frac{g_2}{2\pi} \sinh 2\phi(q) \\
&= \sqrt{\left(v_F + \frac{g_4}{2\pi}\right)^2 - \left(\frac{g_2}{2\pi}\right)^2}
\end{aligned} \tag{4.35}$$

We find that the consistency of the above procedure demands a first constraint to be satisfied

$$(I) \quad |g_2| \leq |2\pi v_F + g_4| \tag{4.36}$$

On the other hand, removing the ultraviolet cutoff implicit in the last term of (4.34) may lead, in general, to a divergent boson ground state energy, unless $\tilde{v}_F - v_F$ goes appropriately to zero at large $|q|$. This finiteness or independence of the ground state energy on the cutoff is not usually seen, though, as very relevant, since even a divergent result may be interpreted as a global shift of the energy scale. It cannot be said the same regarding the normalization of the boson ground state. This is now annihilated by all the “free” operators \tilde{B}_q and is related to the state $|O\rangle_B$ annihilated by the original B_q operators through the expression

$$|O\rangle_{\tilde{B}} \sim \exp\left(\sum_{q>0} \tanh \phi(q) B_q^+ B_{-q}^+\right) |O\rangle_B \tag{4.37}$$

It can be shown that this state is normalizable only if the following constraint is satisfied[4]

$$(II) \quad \lim_{|q|\rightarrow\infty} \sqrt{|q|} \frac{g_2}{2\pi v_F + g_4} = 0 \tag{4.38}$$

We should impose therefore conditions (I) and (II) to ensure the integrability of the Luttinger model. This implies the existence of some length scale which separates the short and long distance ranges in the system. Finally, the condition that both g_2 and g_4 are finite at $q = 0$ is also usually imposed within the context of the Luttinger model. Though it does not arise from the above development, it is needed to maintain the physical properties which characterize the universality class of the model. Its violation, as it happens in the case of the Coulomb interaction, leads in general to new physics, announced by the abnormal behavior of the response functions[9].

To summarize, we have been discussing the Luttinger model, which is actually a class of electronic systems with “density” times “density” type of interactions. The main property of them is that all their excitations can be classified in terms of boson degrees of freedom. Though we have been carrying out the discussion without taking into account the spin, its inclusion leads to the same essential result. This is treated in the following section, where we also complete the bosonization program giving the translation of the electron field in terms of boson operators.

exercise 4.1 Check the equivalence of the representations (4.14) and (4.25) of H_0 .

exercise 4.2 Find the norm of the state (4.37) and the condition for its finiteness.

4.2 Charge-Spin Separation. Luttinger Liquid

In this section we consider the Luttinger model of one-dimensional electrons with spin. The discussion carried out in the previous section for the noninteracting theory can be now entirely reproduced, but the introduction of the spin gives rise to the genuine physical properties that characterize the interacting theory. The most important of them, namely the complete separation of the charge and the spin excitations, builds up the concept of Luttinger liquid. In this universality class should fall one-dimensional systems which may deviate slightly from the Luttinger model description, but share with it the absence of excitations with the same quantum numbers of the electron. This property alone establishes a neat difference with the Fermi liquid behavior characteristic of the higher dimensions.

In order to discuss the above points, the main technical achievement of this section will be the representation of the fermions fields in terms of the boson operators. This involves the rather nontrivial concept of how fermions may arise in a theory built out of bosons[10, 11]. The most clear explanation of this fact is perhaps given by Mandelstam[12]. Once we are able to express every field in terms of the boson fields, we may compute all the correlators of the interacting theory and, in particular, the one-particle electron Green function. Its inspection will clearly show that it lacks the characteristic pole structure of Fermi liquid behavior, proving that in the interacting theory, and no matter how small the strength of the couplings may be, there are no physical states with spin 1/2 and the electron charge. We will finally provide some intuitive picture trying to understand how this deconfinement of the charge and the spin is a plausible phenomenon in one dimension.

4.2.1 Charge-Spin Separation in a Simple Case

The introduction of the spin just amounts to make a parallel counting of the boson excitations for the two spin orientations, in the noninteracting theory. Taking into account (4.25) the expression of the “free” hamiltonian becomes

$$H_0 = \int_0^L dx v_F \frac{\pi}{L^2} (: \rho_{R\uparrow}(x) \rho_{R\uparrow}(x) : + : \rho_{R\downarrow}(x) \rho_{R\downarrow}(x) : + \quad L \leftrightarrow R) \quad (4.39)$$

It is convenient to introduce the respective charge density and spin density fields (we omit the subindices L, R in this formula)

$$\rho(x) = \frac{\rho_{\uparrow}(x) + \rho_{\downarrow}(x)}{\sqrt{2}} \quad , \quad \sigma(x) = \frac{\rho_{\uparrow}(x) - \rho_{\downarrow}(x)}{\sqrt{2}} \quad (4.40)$$

The separation of charge and spin is then manifest in the “free” hamiltonian since

$$H_0 = \int_0^L dx v_F \frac{\pi}{L^2} (: \rho_R(x) \rho_R(x) : + : \sigma_R(x) \sigma_R(x) : + \quad L \leftrightarrow R) \quad (4.41)$$

It can be also shown that in the interacting hamiltonian of the Luttinger model (g_2 and g_4 interactions alone) charge and spin always decouple. Suppose a simple instance in which the interaction is local (apart from some momentum transfer cutoff which we do not write explicitly), involving only the charge density

$$\begin{aligned} H_{int} &= g \frac{1}{L^2} \int_0^L dx : (\rho_L(x) + \rho_R(x)) (\rho_L(x) + \rho_R(x)) : \\ &= g \frac{1}{L^2} \int_0^L dx (: \rho_L(x) \rho_L(x) : + : \rho_R(x) \rho_R(x) :) \\ &\quad + 2g \frac{1}{L^2} \int_0^L dx \rho_L(x) \rho_R(x) \end{aligned} \quad (4.42)$$

The combination $H_0 + H_{int}$ can be diagonalized, as in the previous section, by means of the “pseudorotation”

$$\begin{pmatrix} \rho_L \\ \rho_R \end{pmatrix} = \begin{pmatrix} \cosh \phi & \sinh \phi \\ \sinh \phi & \cosh \phi \end{pmatrix} \begin{pmatrix} \tilde{\rho}_L \\ \tilde{\rho}_R \end{pmatrix} \quad (4.43)$$

For the value

$$\tanh 2\phi = -\frac{g/\pi}{v_F + g/\pi} \quad (4.44)$$

we obtain the diagonal form

$$\begin{aligned} H &= \tilde{v}_F \frac{\pi}{L^2} \int_0^L dx (: \tilde{\rho}_R(x) \tilde{\rho}_R(x) : + L \leftrightarrow R) \\ &\quad + v_F \frac{\pi}{L^2} \int_0^L dx (: \sigma_R(x) \sigma_R(x) : + L \leftrightarrow R) \end{aligned} \quad (4.45)$$

In this example it is quite trivial that the only eigenstates of the hamiltonian are given by spin waves and plasmons. The response functions for charge and spin show the poles corresponding to these physical states, for instance,

$$\begin{aligned} \chi(\omega, k) &\equiv -i \int dt e^{i\omega t} \langle \sigma(t, k) \sigma(0, -k) \rangle \\ &= \frac{v_F^2 k^2}{\omega^2 - v_F^2 k^2 + i\epsilon} \end{aligned} \quad (4.46)$$

The above is just an illustration of the charge-spin separation which *always* takes place in the Luttinger model. It is a good exercise to show that for arbitrary values of $g_{2\parallel}, g_{2\perp}, g_{4\parallel}$ and $g_{4\perp}$ the change of variables (4.40) always decouples the charge and the spin excitations[13]. Then one can perform two independent “pseudorotations” in the respective sectors to bring the hamiltonian to diagonal form, showing that the velocity of spin excitations is different than that of charge excitations, and both different, in general, to v_F .

4.2.2 Boson Representation of Fermion Operators

At first sight it may appear intriguing that a fermion-like object may be built in a theory which, as we have already seen, is made out of bosons. This point is perhaps best understood following Mandelstam[12] and his argumentation about the sine-Gordon model[11]. This is the model for a boson field $\Phi(x)$ with an interaction hamiltonian

$$H_{int} \sim \int dx \cos \Phi(x) \quad (4.47)$$

Together with trivial static solutions like $\Phi(x) = \pm\pi$, the sine-Gordon model has *soliton* solutions which interpolate between different wells of the interaction potential. A single soliton, in particular, complies to the boundary conditions

$$\begin{aligned} \Phi(x) &\rightarrow \pi \quad , \quad x \rightarrow \infty \\ \Phi(x) &\rightarrow -\pi \quad , \quad x \rightarrow -\infty \end{aligned} \quad (4.48)$$

In the quantum theory, therefore, we have two different types of fluctuations. We have particle excitations, which appear by quantizing about the solution $\Phi(x) = \pi$, for instance, and we have also the quanta which arise from the soliton solution. It can be shown that the soliton and the corresponding antisoliton bear nonvanishing fermion number, being therefore the manifestation of the fermion-like object in the theory. This is consistent with our representation (4.23) and (4.24) of the density fluctuations. The total charge of the system (which for the particular sine-Gordon model (4.47) is a conserved charge, see Ref. [12]) is

$$Q = \frac{1}{2\pi} \int_{-\infty}^{+\infty} dx \partial_x \Phi \quad (4.49)$$

which gets nonvanishing (integer) values for the soliton solutions like (4.48). From the point of view of the particles (bosons), the fermion is an object which interpolates between different topological sectors of the model. We will reach a more intuitive understanding of this phenomenon when describing the harmonic chain in Chap. 5.

Following with this argumentation, Mandelstam represents the fermion field $\Psi(x)$ as a soliton *annihilation* operator. That is, it must be an operator which shifts the value of $\Phi(y)$ by 2π to the left of x , and leaves it unmodified to the right. This is expressed in the form

$$[\Phi(y), \Psi(x)] = 2\pi\Psi(x) \quad , \quad y < x \quad (4.50)$$

$$[\Phi(y), \Psi(x)] = 0 \quad , \quad y > x \quad (4.51)$$

A possible representation of $\Psi(x)$ which satisfies these commutation relations is (see (4.20))

$$\Psi(x) =: \mathcal{O}(x) \exp \left(-i2\pi \int^x dy \Pi(y) \right) : \quad (4.52)$$

where the operator $\mathcal{O}(x)$ is still undetermined. If we now require that $\Psi(x)$ and $\Psi(y)$ anticommute at different points x and y , we are led to take the two possibilities[12]

$$\Psi_1(x) = : \exp \left(-i\frac{1}{2}\Phi(x) - i2\pi \int^x dy \Pi(y) \right) : \quad (4.53)$$

$$\Psi_2(x) = : \exp \left(i\frac{1}{2}\Phi(x) - i2\pi \int^x dy \Pi(y) \right) : \quad (4.54)$$

At this point we recognize in the argument of the exponentials the two chiral boson fields (4.21), (4.22). It is therefore appropriate to identify (4.53) and (4.54), respectively, with the two fermion components of given chirality

$$\Psi_R(x) = : \exp (i\Phi_R(x)) : \quad (4.55)$$

$$\Psi_L(x) = : \exp (-i\Phi_L(x)) : \quad (4.56)$$

Quite satisfactorily, it can be also shown that, in a given channel, $\Psi_i(x)$ and $\Psi_i^+(y)$ also satisfy the canonical anticommutation relations

$$\{\Psi_i(x), \Psi_i^+(y)\} = \delta(x - y) \quad i = L, R \quad (4.57)$$

In all these considerations it is implicit the assumption that the fields $\Phi_L(x)$ and $\Phi_R(x)$ are the very same that those defined from the density fields $\rho_L(x)$ and $\rho_R(x)$. There is, however, a nontrivial self-consistency check to be carried out, that is, to verify that the computation of the fermion density for a given channel, $:\Psi_i^+(x)\Psi_i(x):$, with the above boson representation of the fermion fields actually matches the definitions (4.23) and (4.24). This is left as an exercise at the end of the section.

The above boson representation of the chiral fermion fields makes possible the computation of any correlator of the electron system. The full fermion field operator can be decomposed in the form

$$\begin{aligned} \Psi(x) &= \frac{1}{\sqrt{L}} \sum_k e^{ikx} a_k + \frac{1}{\sqrt{L}} \sum_k e^{ikx} b_k \\ &= e^{ik_F x} \frac{1}{\sqrt{L}} \sum_k e^{i(k-k_F)x} a_k + e^{-ik_F x} \frac{1}{\sqrt{L}} \sum_k e^{i(k+k_F)x} b_k \\ &= e^{ik_F x} \Psi_R(x) + e^{-ik_F x} \Psi_L(x) \end{aligned} \quad (4.58)$$

Correlation functions involving any number of Ψ fields can be translated into expectation values on the boson vacuum of products of exponentials of boson fields. The computation requires the knowledge, in general, of the object

$$\langle : e^{i\alpha\Phi(x)} : : e^{-i\alpha\Phi(y)} : \rangle \quad (4.59)$$

In the case $\alpha = 1$, we should recover the free propagator for the chiral fermion with the well-known behavior $\sim (x - y)^{-1}$. As we will see in the next subsection, though, in the interacting theory we get to know the expression (4.59) for arbitrary values of α .

The calculation, for instance, of

$$\langle : e^{i\alpha\Phi_R(x)} : : e^{-i\alpha\Phi_R(y)} : \rangle \quad (4.60)$$

can be accomplished in the following way. In all the pertinent instances, the expectation value refers to the vacuum free of bosons. The way to proceed, then, is to place to the right all the boson annihilation operators. We have already the normal ordered form

$$: \exp(i\alpha\Phi_R(x)) : := \exp\left(-\alpha \sum_{k>0} \sqrt{\frac{2\pi}{kL}} e^{-ikx} B_k^+\right) \exp\left(\alpha \sum_{k>0} \sqrt{\frac{2\pi}{kL}} e^{ikx} B_k\right) \quad (4.61)$$

After use of the formula

$$e^A e^B = e^{B+A} e^{\frac{1}{2}[A,B]} = e^B e^A e^{[A,B]} \quad (4.62)$$

we get

$$\begin{aligned} \langle : e^{i\alpha\Phi_R(x)} : : e^{-i\alpha\Phi_R(y)} : \rangle &= \\ &= \left\langle \prod_{k>0} \exp\left(-\alpha \sqrt{\frac{2\pi}{kL}} e^{-ikx} B_k^+\right) \prod_{p>0} \exp\left(\alpha \sqrt{\frac{2\pi}{pL}} e^{ipx} B_p\right) \times \right. \\ &\quad \left. \prod_{q>0} \exp\left(\alpha \sqrt{\frac{2\pi}{qL}} e^{-iqy} B_q^+\right) \prod_{r>0} \exp\left(-\alpha \sqrt{\frac{2\pi}{rL}} e^{iry} B_r\right) \right\rangle \\ &= \left\langle \prod_{k>0} \exp\left(-\alpha \sqrt{\frac{2\pi}{kL}} e^{-ikx} B_k^+\right) \prod_{q>0} \exp\left(\alpha \sqrt{\frac{2\pi}{qL}} e^{-iqy} B_q^+\right) \times \right. \\ &\quad \left. \prod_{p>0} \exp\left(\alpha \sqrt{\frac{2\pi}{pL}} e^{ipx} B_p\right) \prod_{r>0} \exp\left(-\alpha \sqrt{\frac{2\pi}{rL}} e^{iry} B_r\right) \right\rangle \times \\ &\quad \exp\left(\alpha^2 \frac{2\pi}{pL} e^{ip(x-y)}\right) \\ &= \exp\left(\alpha^2 \frac{2\pi}{L} \sum_{p>0} \frac{1}{p} e^{ip(x-y)}\right) \end{aligned} \quad (4.63)$$

The last expression is more easily evaluated in the infinite volume limit $L \rightarrow \infty$. The sum can be traded then by an integral, taking into account that it is actually regulated in the infrared by the minimum value of the momentum $\Delta \equiv 2\pi/L$,

$$\begin{aligned} \langle : e^{i\alpha\Phi_R(x)} : : e^{-i\alpha\Phi_R(y)} : \rangle &\approx \\ &\approx \exp\left\{\alpha^2 \int_{\Delta}^{\infty} dk \frac{1}{k} e^{ik(x-y)}\right\} \\ &\approx \exp\left\{-\alpha^2 \left[\log(\Delta(x-y)) - i\frac{\pi}{2}\right]\right\} = \left(\frac{L}{2\pi} \frac{i}{(x-y)}\right)^{\alpha^2} \end{aligned} \quad (4.64)$$

This is the final result. In the case of the free electron correlator $\alpha = 1$, it shows the correct spatial behavior, apart from normalization factors. The boson representation of the fermion field needs anyhow to be regulated in the ultraviolet,

and the way we have done it here by the normal order prescription is the usual in quantum field theory[14]. There are, however, more possibilities. In condensed matter physics a more sophisticated prescription is usually taken[10], which allows to reproduce also the imaginary part of the electron Green function (the $i\epsilon$ prescription). This will be used in the description of the discrete models in Chap. 5.

In general, time dependent correlators can be inferred from their static limit, by enforcing the manifest Galilean invariance of the theory. Thus, in the case of a right-handed field the time dependence is obtained replacing $x - x'$ by $x - x' - v_F(t - t')$, while in the case of a left-handed field it amounts to replace $x - x'$ by $x - x' + v_F(t - t')$. This of course can be checked by direct computation with operators in the interaction representation.

4.2.3 Electron Green Function

We illustrate the computation of the electron Green function in the Luttinger model, in the case of the charge density interactions already quoted in (4.42). The general case can be dealt with by means of the same method. We begin by dissociating charge and spin fields (we omit subindices L, R at this point)

$$\Phi_c = \frac{\Phi_\uparrow + \Phi_\downarrow}{\sqrt{2}} \quad , \quad \Phi_s = \frac{\Phi_\uparrow - \Phi_\downarrow}{\sqrt{2}} \quad (4.65)$$

We have, for instance, depending on the orientation of the spin \uparrow or \downarrow

$$\Psi_{R\uparrow} = e^{i(\Phi_{cR} + \Phi_{sR})/\sqrt{2}} \quad (4.66)$$

$$\Psi_{R\downarrow} = e^{i(\Phi_{cR} - \Phi_{sR})/\sqrt{2}} \quad (4.67)$$

We may interpret therefore the electron field as being composed of two completely independent fields, one that carries charge but no spin (the holon) and other that carries spin but no charge (the spinon). This picture is correct to the extent that the hamiltonian is built out of disjoint charge and spin excitations. We may say then that the holon and the spinon are deconfined in one dimension.

What we want to obtain, on the other hand, is a correlator like

$$G_{R\uparrow}(t - t', x - x') = -i \langle T \Psi_{R\uparrow}(t, x) \Psi_{R\uparrow}^\dagger(t', x') \rangle \quad (4.68)$$

in the interacting theory. We could apply for that purpose the expression (4.64), were not for the fact that it is valid only for free fields, as implied in its derivation. It is possible to resort, however, to the linear change of variables (4.43) that decouples left and right modes in the hamiltonian and renders it a diagonal quadratic form in the boson fields. In our case we have to make the canonical transformation

$$\begin{pmatrix} \Phi_{cL} \\ \Phi_{cR} \end{pmatrix} = \begin{pmatrix} \cosh \phi & \sinh \phi \\ \sinh \phi & \cosh \phi \end{pmatrix} \begin{pmatrix} \tilde{\Phi}_{cL} \\ \tilde{\Phi}_{cR} \end{pmatrix} \quad (4.69)$$

to obtain free fields $\tilde{\Phi}_{cL}$ and $\tilde{\Phi}_{cR}$. Φ_{sL} and Φ_{sR} are already decoupled, but in the general case with spin-dependent interactions another ‘‘pseudorotation’’ to free fields may be needed in the spin sector. By playing with the holon-spinon decomposition and the decoupling of left and right modes, the interacting electron Green function reduces to a product of correlators of the type (4.64).

Without paying attention to normalization factors, we have

$$\begin{aligned}
G_{R\uparrow}(t-t', x-x') &= \\
&= \langle e^{i(\Phi_{cR}(t,x)+\Phi_{sR}(t,x))/\sqrt{2}} e^{-i(\Phi_{cR}(t',x')+\Phi_{sR}(t',x'))/\sqrt{2}} \rangle \\
&= \langle e^{i\Phi_{cR}(t,x)/\sqrt{2}} e^{-i\Phi_{cR}(t',x')/\sqrt{2}} \rangle \langle e^{i\Phi_{sR}(t,x)/\sqrt{2}} e^{-i\Phi_{sR}(t',x')/\sqrt{2}} \rangle \\
&= \langle e^{i\Phi_{cR}(t,x)/\sqrt{2}} e^{-i\Phi_{cR}(t',x')/\sqrt{2}} \rangle \frac{1}{|x-x'-v_F(t-t')|^{1/2}} \tag{4.70}
\end{aligned}$$

where we have made use of (4.64) for the spinon operators. The charge correlator requires first the transformation to decoupled holon fields. Abbreviating $\sinh\phi \equiv s$ and $\cosh\phi \equiv c$, we have

$$\begin{aligned}
G_{R\uparrow}(t-t', x-x') &= \\
&= \langle e^{i(s\tilde{\Phi}_{cL}(t,x)+c\tilde{\Phi}_{cR}(t,x))/\sqrt{2}} e^{-i(s\tilde{\Phi}_{cL}(t',x')+c\tilde{\Phi}_{cR}(t',x'))/\sqrt{2}} \rangle \times \\
&\quad \frac{1}{|x-x'-v_F(t-t')|^{1/2}} \\
&= \langle e^{is\tilde{\Phi}_{cL}(t,x)/\sqrt{2}} e^{-is\tilde{\Phi}_{cL}(t',x')/\sqrt{2}} \rangle \langle e^{ic\tilde{\Phi}_{cR}(t,x)/\sqrt{2}} e^{-ic\tilde{\Phi}_{cR}(t',x')/\sqrt{2}} \rangle \times \\
&\quad \frac{1}{|x-x'-v_F(t-t')|^{1/2}} \\
&= \frac{1}{|x-x'+\tilde{v}_F(t-t')|^{s^2/2}} \frac{1}{|x-x'-\tilde{v}_F(t-t')|^{c^2/2}} \times \\
&\quad \frac{1}{|x-x'-v_F(t-t')|^{1/2}} \tag{4.71}
\end{aligned}$$

where \tilde{v}_F is, from (4.35),

$$\tilde{v}_F = \sqrt{\left(v_F + \frac{g}{\pi}\right)^2 - \left(\frac{g}{\pi}\right)^2} \tag{4.72}$$

The final result can be written in the form

$$\begin{aligned}
G_{R\uparrow}(t-t', x-x') &= \\
&= \frac{1}{|x-x'-\tilde{v}_F(t-t')|^{1/2}} \frac{1}{|x-x'-v_F(t-t')|^{1/2}} \times \\
&\quad \frac{1}{|(x-x')^2 - \tilde{v}_F^2(t-t')^2|^{s^2/2}} \tag{4.73}
\end{aligned}$$

The effect of the separation of charge and spin is manifest in the electron Green function, since the two different velocities v_F and \tilde{v}_F account for the different

propagation speed of charge and spin excitations. It is also remarkable that the propagation of the fermion field $\Psi_{R\uparrow}$ is not purely in the right direction, as far as $s^2 \neq 0$. The same admixture is also found in the propagator of the left-handed fermion, which is obtained from (4.73) by replacing $v_F \rightarrow -v_F$ and $\tilde{v}_F \rightarrow -\tilde{v}_F$. This lack of perfect propagation in a given direction can be interpreted on physical grounds by the fact that fermions of a given chirality excite, in its propagation, the fermions of the opposite chirality. Thus, there is a phenomenon of “reflection”, by which we always find the superposition of two waves travelling in opposite directions.

Though the electron Green function has the simplest expression in (t, x) space, the physical properties related to the spectrum have to be addressed in momentum representation. The above propagator (4.73) does not admit a simple expression in (ω, k) space, but one may still obtain the Fourier transform of the factors and write that of the product as a convolution operation. The Fourier transform of (4.73) becomes then[15]

$$G_{R\uparrow}(\omega, k) \sim \frac{1}{|(\tilde{v}_F k - \omega)(v_F k - \omega)|^{1/2}} * (\tilde{v}_F^2 k^2 - \omega^2)^{s^2/2-1} \quad (4.74)$$

where $*$ symbolically denotes the convolution product. The corresponding expression for the left-handed fermion is obtained again by the replacements $v_F \rightarrow -v_F$ and $\tilde{v}_F \rightarrow -\tilde{v}_F$. The conclusion that we get by inspection of (4.74) is that we do not find fermion excitations after looking for poles of the fermion propagator. Actually, for a given value of the momentum this object has branch cuts instead of poles. This absence of fermion states in the spectrum is not surprising since, after all, we had already classified the physical states into bosonic charge and spin excitations. These certainly do appear as poles of the corresponding response functions for charge and spin operators.

The above result is very important since it shows that the Luttinger model is the prototype for a quite different liquid than that dealt with in Landau's Fermi liquid theory. In fact, we may characterize this universality class, called by the name of Luttinger liquid[4], by the breakdown of the quasiparticle picture. No matter how small the strength of the interaction may be, all trace of quasiparticle poles disappears in the electron Green function, and no physical states remain with the same quantum numbers of the electron.

Another distinctive signal not shared by the Fermi liquid arises from the behavior of the momentum distribution function $n(k)$ at the Fermi level. This is again a consequence of the particular form of the correlator (4.74). $n(k)$ is defined about k_F by

$$n(k) = -i \lim_{t \rightarrow 0^-} \int_{-\infty}^{+\infty} dx e^{-i(k-k_F)x} G_R(t, x) \quad (4.75)$$

In Fermi liquid theory the small imaginary part of the Green function at the quasiparticle pole leads to the well-known discontinuity of $n(k)$ at the Fermi level. Now the presence of the branch cut changes the nature of the singularity. In order to apply correctly (4.75) we need the precise knowledge of the complex

structure of $G_R(t, x)$. This can be found in Ref. [3]. The limit $t \rightarrow 0^-$ fixes the imaginary part of the Green function

$$G_R(0^-, x) = \frac{1}{2\pi} \frac{1}{x - i\delta} \frac{1}{(\Lambda^2 (x - i\Lambda^{-1})(x + i\Lambda^{-1}))^{s^2/2}} \quad (4.76)$$

where δ^{-1} is a bandwidth cutoff and Λ is a momentum transfer cutoff in the interaction. By introducing this expression in (4.75) we find

$$\begin{aligned} n(k) &= -i \frac{1}{2\pi} \int_{-\infty}^{+\infty} dx e^{-i(k-k_F)x} \frac{1}{x - i\delta} \frac{1}{(\Lambda^2 x^2 + 1)^{s^2/2}} \\ &= \frac{1}{2} \int_{-\infty}^{+\infty} dx e^{-i(k-k_F)x} \delta(x) \frac{1}{(\Lambda^2 x^2 + 1)^{s^2/2}} \\ &\quad - \frac{1}{2\pi} \text{PP} \int_{-\infty}^{+\infty} dx \frac{\sin(k - k_F)x}{x} \frac{1}{(\Lambda^2 x^2 + 1)^{s^2/2}} \\ &\approx \frac{1}{2} - \text{const.} |k - k_F|^{s^2} \text{sgn}(k - k_F) \end{aligned} \quad (4.77)$$

A symmetric expression holds about the other Fermi point at $-k_F$. We see that the jump in the momentum distribution function, which in the Fermi liquid equals the residue of the quasiparticle pole, has disappeared. Instead we have a continuous function, though with infinite slope at the Fermi points. This allows us, in a certain sense, to maintain the notion of Fermi level in the Luttinger liquid, as the level at which the derivative of $n(k)$ becomes infinite.

4.2.4 Intuitive Picture of Charge-Spin Separation

To close this section and the chapter, we try to give here an intuitive explanation of the phenomenon of separation of charge and spin in one dimension. Suppose, for instance, that we have a periodic disposition of electrons, with antiferromagnetic order, as shown in Fig. 4.2(a). This cannot represent a physical state of our one-dimensional theory but we may consider it as a local picture, pertinent to the ground state of systems like the one-dimensional Hubbard model. It represents a state free of spin and charge excitations. Suppose now that we introduce a hole in the system, which amounts to remove the charge and the spin at a given site of the periodic disposition (Fig. 4.2(b)). If we exchange the empty site with its neighbor to the left, after repeated application of this operation we observe that two different kinds of perturbation have been introduced in the system. We end up with the empty site, which does not disturb the antiferromagnetic order, and with a ‘‘domain wall’’ (the two consecutive spins pointing up) representing a frustration of the order (Fig. 4.2(c)). Obviously this frustration can be also propagated by exchanging neighboring spins at one side of the wall. Thus, we have the picture of two different perturbations of the original configuration, free to evolve one independently of the other. The first corresponds to what we called ‘‘holon’’ in the mathematical framework, while the second is the image of

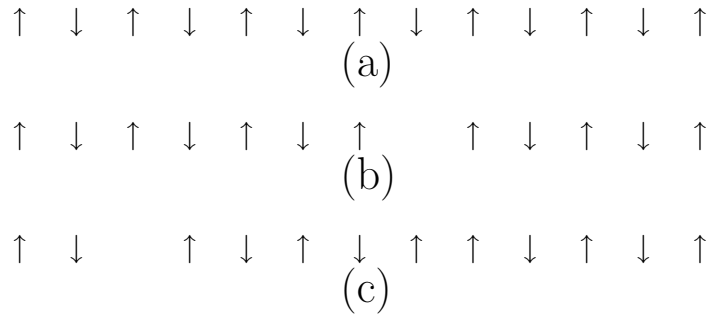


Fig. 4.2. Sequence of events showing the creation of a hole and a domain wall of the antiferromagnetic order.

the “spinon” excitation. This simple picture makes plausible that the “holon” and the “spinon” may be disjoint excitations, able to propagate each of them with its own velocity. It also stresses to what extent the dimensionality of the system is crucial to understand the phenomenon of charge and spin separation. One can readily see that any attempt to implement this picture in two dimensions is not going to work out with the simplicity shown here. The question of whether there can be two-dimensional systems with the property of charge-spin separation similar to that of the Luttinger liquid is nowadays the subject of a big debate.

exercise 4.3 Check that in the most general Luttinger model with $g_{2\parallel}$, $g_{2\perp}$, $g_{4\parallel}$ and $g_{4\perp}$ interactions the hamiltonian splits into two respective parts for charge and spin operators.

exercise 4.4 Compute the fermion density operator : $\Psi_R^\dagger(x)\Psi_R(x)$: using the boson representation of the fermion field and compare with the former definition (4.24).

References

- [1]S. Tomonaga, *Prog. Theor. Phys.* **5** (1950) 349.
- [2]J. M. Luttinger, *J. Math. Phys.* **4** (1963) 1154.
- [3]I. E. Dzyaloshinsky and A. I. Larkin, *Soviet Phys. JETP* **38** (1974) 202.
- [4]F. D. M. Haldane, *J. Phys. C* **14** (1981) 2585.
- [5]G. D. Mahan, *Many Particle Physics* (Plenum, New York, 1981).
- [6]A. Luther and K. D. Schotte, *Nucl. Phys. B* **242** (1984) 407.
- [7]D. Minic, *Mod. Phys. Lett. B* **7** (1993) 641.
- [8]D. C. Mattis and E. H. Lieb, *J. Math. Phys.* **6** (1965) 304.
- [9]H. J. Schulz, *Phys. Rev. Lett.* **71** (1993) 1864.
- [10]A. Luther and I. Peschel, *Phys. Rev. B* **9** (1974) 2911.
- [11]S. Coleman, *Phys. Rev. D* **11** (1975) 2088.
- [12]S. Mandelstam, *Phys. Rev. D* **11** (1975) 3026.
- [13]J. Sólyom, *Adv. Phys.* **28** (1979) 201.
- [14]A. M. Polyakov, *Gauge Fields and Strings*, Chap. 9 (Harwood, London, 1989).
- [15]X. G. Wen, *Phys. Rev. B* **42** (1990) 6623.

5. Correspondence from Discrete to Continuum Models

5.1 Introduction

We have seen in the preceding chapter that the bosonization technique is a very powerful tool for studying one-dimensional electron systems. We have uncovered with it the properties of a continuous set of models showing critical behavior and governing the low-energy physics of a wide region of the parameter space of all the theories. The very fact of describing a number of critical properties is actually what justifies the study accomplished in the continuum limit. One may think that the assumption of an infinite linear dispersion relation for the electrons is a crucial step in the rigorous proof of the boson-fermion correspondence and wonder to what extent the results obtained by means of the bosonization program may apply to more realistic models. In particular, any model of fermions hopping on a lattice must have a compact dispersion relation of the kind shown in Fig. 3.1. There is empirical evidence, though, that the presence of the lattice does not change essentially the low-energy properties and that the Luttinger liquid paradigm continues applying to a wide class of discrete models. Some of these can be studied analytically by means of the Bethe ansatz technique, which provides exact results for the energy spectrum and some thermodynamic quantities. The case of the Hubbard model, for instance, is treated with detail in Chap. 10. From the exact resolution of the models one also gets information about the mapping to the Luttinger liquid universality class. This amounts to the knowledge of the parameters which characterize the model within the line of critical points obtained in Chap. 3. Thus, different systems like the antiferromagnetic Heisenberg chain, the spinless fermion model into which the former can be mapped or the Hubbard model at weak coupling have a low-energy behavior dictated by points over the critical line. The effect of the lattice only shows up in the form of certain renormalization of the parameters determining the critical point. Most significantly, it turns out that the correspondence to the mentioned universality class holds even in the presence of strong interactions, as is the case of the harmonic chain or the Hubbard model in the limit of large on-site repulsion. We will discuss these two models in what follows. The correspondence with the continuum approach has important consequences from a practical point of view, since it allows to ascertain low-energy

properties like the charge-spin separation and the long-distance behavior of the correlation functions in the discrete models. These are not obtained by the exact Bethe ansatz resolution and, in most cases, are not susceptible either of an accurate numerical determination with the present computational techniques.

5.2 The Harmonic Chain

The first example of discrete one-dimensional model that we consider is the harmonic chain, which is essentially a system of particles tied by a nearest-neighbor harmonic oscillator potential[1]. This model does not seem to bear, at first sight, a direct relation with the continuum electron systems discussed previously, but it actually provides a good description of the electron liquid when there are strong correlation effects. This is the case of the large- U limit of the Hubbard model that we will discuss further on. In that extreme situation only the charge dynamics becomes nontrivial in the low-energy limit, and it can be modeled by some elastic coupling provided by the holes between adjacent electrons in the lattice. A most important point is that the continuum limit of the harmonic chain adopts the same form that the boson representation of the Luttinger model. This gives a clear indication that systems in the strong coupling regime may fall into the Luttinger universality class. The harmonic chain will also serve us to reach a more intuitive understanding of the boson description of one-dimensional electron systems.

5.2.1 Continuum Limit

We start with a system of N particles whose first-quantized hamiltonian is

$$H = \sum_{n=1}^N \left\{ \frac{P_n^2}{2m} + \frac{\lambda}{2} (X_{n+1} - X_n - d)^2 \right\} \quad (5.1)$$

Thus, the particles X_n and X_{n+1} suffer a repulsive interaction at short distances, while they reach a most stable configuration at a relative distance d . The quantum properties of the model are best investigated in the continuum limit $d \rightarrow 0$ [1]. Then the label n is promoted to a continuous variable $x = nd$ while the position of each particle is expanded about the classical configuration, so that

$$nd \rightarrow x \quad (5.2)$$

$$X_n \rightarrow nd + \frac{1}{2\pi} d \Phi(x) \quad (5.3)$$

$$P_n \rightarrow 2\pi \Pi(x) \quad (5.4)$$

The fields $\Phi(x)$ and $\Pi(x)$ satisfy the canonical commutation relation

$$[\Phi(x), \Pi(y)] = i\delta(x - y) \quad (5.5)$$

On the other hand, we have

$$X_{n+1} - X_n - d \rightarrow \frac{1}{2\pi} d^2 \partial_x \Phi \quad (5.6)$$

The hamiltonian in the continuum limit becomes

$$\begin{aligned} H &= \frac{1}{2m} \frac{1}{d} 4\pi^2 \int dx \Pi^2(x) + \frac{1}{2} \lambda d^3 \frac{1}{4\pi^2} \int dx (\partial_x \Phi(x))^2 \\ &= \frac{v}{2} \int dx \left\{ 4\pi\mu \Pi^2(x) + \frac{1}{4\pi\mu} (\partial_x \Phi(x))^2 \right\} \end{aligned} \quad (5.7)$$

with the parameters

$$v = d \sqrt{\frac{\lambda}{m}} \quad , \quad \mu = \frac{1}{d^2} \frac{\pi}{\sqrt{\lambda m}} \quad (5.8)$$

The model is therefore completely specified by the velocity v and the dimensionless parameter μ . We will see afterwards that the latter gives a measure of the strength of the quantum fluctuations, the classical limit being approached as $\mu \rightarrow 0$.

In order to bring the hamiltonian to the canonical free boson form (4.25), one may perform the transformation

$$\begin{aligned} \Phi(x) &= \sqrt{\mu} \tilde{\Phi}(x) \\ \Pi(x) &= \frac{1}{\sqrt{\mu}} \tilde{\Pi}(x) \end{aligned} \quad (5.9)$$

which, obviously, preserves the canonical commutation relations. In fact, this is nothing but the real-space version of the Bogoliubov transformation in (4.31) and (4.32), that we introduced to diagonalize the boson expression of the Luttinger model hamiltonian. Recalling (4.18) and (4.19), we may cast the above transformation in the already familiar form

$$\begin{pmatrix} \Phi_L \\ \Phi_R \end{pmatrix} = \begin{pmatrix} \frac{1}{2}(\sqrt{\mu} + \frac{1}{\sqrt{\mu}}) & \frac{1}{2}(\sqrt{\mu} - \frac{1}{\sqrt{\mu}}) \\ \frac{1}{2}(\sqrt{\mu} - \frac{1}{\sqrt{\mu}}) & \frac{1}{2}(\sqrt{\mu} + \frac{1}{\sqrt{\mu}}) \end{pmatrix} \begin{pmatrix} \tilde{\Phi}_L \\ \tilde{\Phi}_R \end{pmatrix} \quad (5.10)$$

which draws the relation between μ and the rotation angle ϕ of the Bogoliubov transformation

$$\cosh \phi \leftrightarrow \frac{1}{2} \left(\sqrt{\mu} + \frac{1}{\sqrt{\mu}} \right) \quad (5.11)$$

In the present model one is mainly interested in the correlators of the density operator $\rho(x)$. In terms of the discrete variables, this is written in the form

$$\begin{aligned} \rho(x) &= \sum_{n=1}^N \delta(x - X_n) \\ &= \int_{-\infty}^{+\infty} \frac{dq}{2\pi} \sum_{n=1}^N e^{iq(x-X_n)} \end{aligned} \quad (5.12)$$

If we make the passage to the $\Phi(x)$ field variable we get

$$\rho(x) = \int_{-\infty}^{+\infty} \frac{dq}{2\pi} e^{iqx} \sum_{n=1}^N e^{-iqdn} e^{-iqd\Phi/(2\pi)} \quad (5.13)$$

A crucial assumption is that the Φ field accounts for a smooth quantum fluctuation effect. In that case the sum over n has a significant value only for $q \approx 2\pi m/d, m = 0, \pm 1, \pm 2, \dots$. In the continuum limit we get a contribution about each of these dominant momenta

$$\rho(x) = \sum_{m=-\infty}^{+\infty} e^{i2\pi mx/d} \rho_m(x) \quad (5.14)$$

For $m \neq 0$ we have

$$\rho_m(x) \approx \frac{1}{d} e^{im\Phi(x)} \quad (5.15)$$

The $m = \pm 1$ contributions correspond to the well-known chirality-mixing density fluctuations near $2k_F$. In fact, for fermions without spin this quantity equals 2π over the mean separation between particles. What we learn here is that under strong correlation effects, as they occur in the harmonic chain, we may expect density fluctuations about any integer multiple of $2k_F$. We may think of this phenomenon in the same way we understand the Bragg diffraction in a lattice, though it is clear that in the present model we cannot have long-range order regarding the position of the particles. The square of the relative displacement between these diverges logarithmically with their distance, according to the two-point correlator of the boson field.

On the other hand, for $m = 0$, $\rho_0(x)$ is the uniform density of the chain. In the original discrete variables this quantity is $1/(X_{n+1} - X_n)$, which in the continuum limit becomes

$$\rho_0(x) \approx \frac{1}{d + d^2 \frac{1}{2\pi} \partial_x \Phi} \approx \frac{1}{d} - \frac{1}{2\pi} \partial_x \Phi \quad (5.16)$$

We recover in this way the expression of the uniform density $\rho_L + \rho_R$ in terms of the boson field $\Phi = \Phi_L + \Phi_R$. We see, moreover, the explicit appearance of the constant mode $1/d$, which is nothing but the mean particle density of the chain. It corresponds to the contribution from the Fermi sea in the Luttinger model, which we conveniently subtracted out in the definition of the charges N_L and N_R . To summarize, the above description makes clear that there is a correspondence of the dynamics and the observables of the harmonic chain to those of the boson representation of the Luttinger model[1]. There are higher harmonic effects from the contributions (5.15), which arise from the discrete character of the model and survive in the continuum limit, but we may conclude that the physical properties of the harmonic chain are essentially the same as those configuring the Luttinger liquid universality class.

5.2.2 Correlation Functions

The correlators of the density field $\rho(x)$ are significant observables in the harmonic chain. According to the decomposition (5.14), in the two-point density

correlator we may expect oscillations of any multiple of $2\pi/d$. Each of these contributions is given by the vacuum expectation value of the product of two exponentials of the type (5.15). After making the transformation (5.9) to free fields, one could resort again to the computational technique developed for the electron Green function in the Luttinger model. Here, however, we want to follow the same steps but implementing a different regularization, better suited to the discrete character of the model. Instead of dealing with the normal order prescription for the exponential of the field, we make use of the fact that the model describes fluctuations about a mean separation d between neighboring particles. Thus, in the mode expansion of the boson field $\Phi(x)$ there is a built-in short-distance cutoff, which we can make explicit by introducing a factor $\exp(-\epsilon|k|/2)$, with $\epsilon \equiv d/(2\pi)$, in the sum over momenta. Following the same strategy as in (4.63), we get for a typical, say right-handed, free-field correlator

$$\begin{aligned}
& \langle e^{i\alpha\Phi_R(x)} e^{-i\alpha\Phi_R(y)} \rangle = \\
& = \langle \exp\left(-\alpha \int_{\Delta}^{\infty} \frac{dk}{\sqrt{k}} e^{-\epsilon k/2} e^{-ikx} B_k^+\right) \exp\left(\alpha \int_{\Delta}^{\infty} \frac{dp}{\sqrt{p}} e^{-\epsilon p/2} e^{ipx} B_p\right) \times \\
& \quad \exp\left(\alpha \int_{\Delta}^{\infty} \frac{dq}{\sqrt{q}} e^{-\epsilon q/2} e^{-iqy} B_q^+\right) \exp\left(-\alpha \int_{\Delta}^{\infty} \frac{dr}{\sqrt{r}} e^{-\epsilon r/2} e^{iry} B_r\right) \rangle \times \\
& \quad \exp\left(-\frac{\alpha^2}{2} \int_{\Delta}^{\infty} \frac{dp}{p} e^{-\epsilon p}\right) \exp\left(-\frac{\alpha^2}{2} \int_{\Delta}^{\infty} \frac{dr}{r} e^{-\epsilon r}\right) \\
& = \langle \exp\left(-\alpha \int_{\Delta}^{\infty} \frac{dk}{\sqrt{k}} e^{-\epsilon k/2} e^{-ikx} B_k^+\right) \exp\left(\alpha \int_{\Delta}^{\infty} \frac{dq}{\sqrt{q}} e^{-\epsilon q/2} e^{-iqy} B_q^+\right) \times \\
& \quad \exp\left(\alpha \int_{\Delta}^{\infty} \frac{dp}{\sqrt{p}} e^{-\epsilon p/2} e^{ipx} B_p\right) \exp\left(-\alpha \int_{\Delta}^{\infty} \frac{dr}{\sqrt{r}} e^{-\epsilon r/2} e^{iry} B_r\right) \rangle \times \\
& \quad \exp\left(\alpha^2 \int_{\Delta}^{\infty} \frac{dp}{p} e^{-\epsilon p} e^{ip(x-y)}\right) \exp\left(-\alpha^2 \int_{\Delta}^{\infty} \frac{dp}{p} e^{-\epsilon p}\right) \\
& = \exp\left(-\alpha^2 \int_{\Delta}^{\infty} \frac{dp}{p} e^{-\epsilon p} (1 - e^{ip(x-y)})\right) \tag{5.17}
\end{aligned}$$

We have performed the computation in the limit of an infinite chain ($L \rightarrow \infty$). Consequently, we can set $\Delta = 0$ as the integral inside the exponential is well-behaved in the infrared. The ϵ parameter regulates it in the ultraviolet, giving the result

$$\begin{aligned}
\langle e^{i\alpha\Phi_R(x)} e^{-i\alpha\Phi_R(y)} \rangle & = \exp\left(-\alpha^2 \log(1 - i(x-y)/\epsilon)\right) \\
& = (\epsilon)^{\alpha^2} \left(\frac{i}{x-y+i\epsilon}\right)^{\alpha^2} \tag{5.18}
\end{aligned}$$

It is worthwhile to compare the result (5.18) with that in (4.64) obtained with the field theory prescription. Using the latter, the exponentials of the boson fields get effective dimensions with respect to the length L of the system. By using the discrete approach, the dimensions are given in terms of the chain

spacing $d \equiv 2\pi\epsilon$. One may think that one method is dual of the other, but the agreement between the spatial dependences in both cases shows that they are simply different ways of extracting the long-distance behavior of the correlator.

Putting together the left-handed and right-handed factors, we finally have for a typical contribution to the density-density correlator

$$\begin{aligned} \langle \rho_m(x) \rho_{-m}(y) \rangle &= \frac{1}{d^2} \langle e^{im\tilde{\Phi}(x)} e^{-im\tilde{\Phi}(y)} \rangle \\ &= \frac{1}{d^2} \langle e^{im\sqrt{\mu}\tilde{\Phi}(x)} e^{-im\sqrt{\mu}\tilde{\Phi}(y)} \rangle \\ &= \left(d^2\right)^{m^2\mu-1} \left(\frac{1}{4\pi^2} \frac{1}{(x-y)^2}\right)^{m^2\mu} \end{aligned} \quad (5.19)$$

The power-law decay of the correlators is a reflection of the critical behavior of the model. The critical properties are however non-universal since they depend on the interaction strength. We are thus describing a continuous line of critical points labeled by the μ parameter.

The space-time dependence of the correlators can be inferred from that of the chiral factors to obtain

$$\langle \rho_m(t, x) \rho_{-m}(t', y) \rangle = \left(d^2\right)^{m^2\mu-1} \left(\frac{1}{4\pi^2} \frac{1}{(x-y)^2 - v^2(t-t')^2}\right)^{m^2\mu} \quad (5.20)$$

The Fourier transform of the density-density correlator is the dynamical structure factor of the model $S(\omega, k)$ [1]. About $k = 2\pi m/d$, this is given by the Fourier transform of the expression (5.20), that is,

$$S(\omega, 2\pi m/d + q) \sim \left(d^2\right)^{m^2\mu-1} \left|\omega^2 - v^2 q^2\right|^{m^2\mu-1} \quad (5.21)$$

On the other hand, the Fourier transform of the equal-time density-density correlator gives the X-ray structure factor $S(k)$ [1], which is made of a sum of contributions about $2\pi m/d$

$$S(2\pi m/d + q) \sim \left(d^2\right)^{m^2\mu-1} |q|^{2m^2\mu-1} \quad (5.22)$$

In this object we find the first divergence only for $\mu < 1/2$. In the classical model, $S(k)$ is given at zero temperature by a sum of delta function peaks, reflecting the perfect order of the chain. In the quantum theory, this long-range order is replaced by the tendency to order (“quasi” long-range order) that the power-law singularity in equation (5.22) shows. It becomes clear that the parameter μ provides a measure of the strength of the quantum fluctuations. The correlations become weaker for greater values of μ , when the singularities in $S(k)$ disappear and the system resembles more a gas. On the contrary, the classical limit is attained when $\mu \rightarrow 0$, as more and more peaks appear in the X-ray structure factor.

5.2.3 Massive Interactions

The harmonic chain in the continuum limit is governed by the line of critical points forming the Luttinger liquid universality class. In fact, it has helped us to give a more concrete meaning to some of the objects that we introduced in the description of the Luttinger model. Thus, we have visualized the $\Phi(x)$ field as a displacement of the particles about the equilibrium position, and we have obtained the $2k_F$ oscillation in the density correlator as an effect due to the quasiperiodic character of the system. As in the Luttinger model, it is clear that the harmonic chain becomes a system without a gap in the excitation spectrum, in the thermodynamic limit $N \rightarrow \infty$. One may ask, however, whether there is any relevant interaction which may drive the model out of criticality.

In order to answer this question one has to incorporate the lattice substrate which is supposed to support the chain of particles. That is, the description of the chain has not implied up to now any consideration about the crystal lattice underlying the system. The periodicity of this lattice may not bear any relation with the mean distance d between the particles. However, when there is commensuration, i.e. when $2\pi m/d$ equals the length G of a vector of the reciprocal lattice, Umklapp processes appear in which the momentum of the particles is absorbed by the crystal. In the first instance $m = 1$, we have an interaction of the type

$$\begin{aligned} H_U &= \frac{1}{2} \frac{g_U}{d} \int dx (\rho_1(x) + \rho_{-1}(x)) \\ &= \frac{g_U}{d^2} \int dx \cos \Phi(x) \end{aligned} \quad (5.23)$$

The field theory takes the form of the well-known sine-Gordon model, that we already introduced in Chap. 4. In the quantum theory all the excited states of this model are massive. In particular, the low-energy excitations are either small fluctuations about any of the minima of the potential or soliton-like excitations in which the $\Phi(x)$ field goes from one to other of the minima.

We have already seen in Chap. 4 that the soliton-like objects have fermionic character. In the present context we may understand this in the following way. A soliton which complies with the boundary conditions

$$\begin{aligned} \Phi(x) &\rightarrow \pi \quad , \quad x \rightarrow \infty \\ \Phi(x) &\rightarrow -\pi \quad , \quad x \rightarrow -\infty \end{aligned} \quad (5.24)$$

is an object that, according to (5.3), represents a progressive relative displacement of the particles of the chain going from left to right. The particle placed to the extreme right is shifted a relative distance d to the right with respect to that at the extreme left. This is like having effectively one particle less in the chain. Similarly, the antisoliton complying with the boundary conditions

$$\begin{aligned} \Phi(x) &\rightarrow -\pi \quad , \quad x \rightarrow \infty \\ \Phi(x) &\rightarrow \pi \quad , \quad x \rightarrow -\infty \end{aligned} \quad (5.25)$$

appears like having in the average one more particle in the chain.

As stated before, the soliton-like excitations have a nonvanishing mass in the quantum theory. After performing the canonical transformation (5.9), the complete hamiltonian of the field theory becomes

$$H = \frac{v}{2} \int dx \left\{ 4\pi \tilde{\Pi}^2(x) + \frac{1}{4\pi} (\partial_x \tilde{\Phi}(x))^2 \right\} + \frac{g_U}{d^2} \int dx \cos(\sqrt{\mu} \tilde{\Phi}(x)) \quad (5.26)$$

The quantum theory is unambiguously defined only for $\mu < 2$ (check this constraint with the different normalization used in Ref. [2]). At $\mu = 1$, for instance, the model is equivalent to a theory of free Dirac massive fermions. We may arrive at this conclusion by using the boson representation (4.55),(4.56) of the two fermion chiralities (see also (5.34) and (5.35)). For the above value we have

$$\begin{aligned} \frac{1}{d^2} \int dx \cos \tilde{\Phi}(x) &= \frac{1}{2} \frac{1}{d^2} \int dx \left(e^{i(\tilde{\Phi}_L + \tilde{\Phi}_R)} + \text{h. c.} \right) \\ &\sim \frac{1}{2} \frac{1}{d} \int dx \left(\Psi_L^+ \Psi_R + \Psi_R^+ \Psi_L \right) \end{aligned} \quad (5.27)$$

which is nothing but the mass term of a one-dimensional relativistic fermion theory. For $\mu < 2$, the last term in (5.26) is in general a relevant perturbation of the critical theory. This can be seen by noticing that, if one were to treat it as a weak interaction, one would face in a perturbative computation the appearance of correlators of the form

$$\frac{1}{d^4} \langle \cos(\sqrt{\mu} \tilde{\Phi}(x)) \cos(\sqrt{\mu} \tilde{\Phi}(y)) \rangle \sim \frac{1}{d^4} \left(\frac{d^2}{(x-y)^2} \right)^\mu \quad (5.28)$$

which diverge in the limit $d \rightarrow 0$ as far as $\mu < 2$.

As a consequence of the gap in the excitation spectrum, systems in which the charge is commensurate with the lattice spacing are genuine insulators. Only upon doping do fermion kinks (the soliton-like objects) appear in the ground state configuration, that is the way in which the system may transport charge. The brief account carried out here stresses the relevance of the lattice effects in the metal-insulator transition in one-dimensional systems, which is a topic extensively treated in the literature[3].

5.3 The Hubbard Model

The Hubbard model is the prototype of a system in which the emphasis is placed on correlation effects between the electrons. In one dimension the model can be solved exactly[4], the meaning of this being that the energy of the ground state and of the excited states can be obtained through a system of coupled nonlinear equations. The exact resolution of the model by the Bethe ansatz technique is reviewed in Chap. 10. Here we rather want to work out the continuum limit of the model, in the instances in which this may be feasible. The reason of this approach to the problem is that, being the interaction purely on-site on the

lattice, we should expect a simple field theory governing the continuum limit and, therefore, the low-energy properties of the discrete model. This description in terms of continuous field variables is of the utmost interest, since the Bethe ansatz technique does not shed light on the long-distance behavior of the correlation functions. It turns out, however, that the continuum limit of the model is not so straightforward as in the case of the harmonic chain, for instance, and that it can be easily established only in the extreme situations of weak coupling[5] and large on-site repulsion[6, 7]. In the latter case, the procedure is somewhat heuristic and combines information from the ground state wavefunction in the large- U limit and from numerical results. A different line of research has been pursued by applying finite size scaling to the low-energy data obtained by the Bethe ansatz approach[8, 9]. In this way, a correspondence between the low-energy excitations in the spectrum and the fields of two independent $c = 1$ conformal field theories has been drawn. This development has been also used in the determination of several critical exponents, with apparent success.

5.3.1 Weak Coupling

The Hubbard model in one dimension is given by the hamiltonian

$$H = -t \sum_{i,\sigma} \left(a_{i,\sigma}^+ a_{i+1,\sigma} + \text{h. c.} \right) + U \sum_i n_{i\uparrow} n_{i\downarrow} \quad (5.29)$$

where $a_{i,\sigma}^+$, $a_{i,\sigma}$ are fermion creation and annihilation operators and $n_{i,\sigma}$ is the number operator at site i for spin $\sigma = \uparrow, \downarrow$. We will be concerned all the time with the case of repulsive interaction ($U > 0$). When the on-site repulsion U is not very large (compared to t), we may expect not very strong correlation effects and that a sensible continuum limit can be worked out from the microscopic hamiltonian.

The kinetic part of the hamiltonian poses no problem in that respect. Following the same steps as in the beginning of Chap. 3, we may introduce a fermion field at each of the two Fermi points in the limit in which the lattice spacing a goes to zero, that is,

$$a_n \rightarrow e^{-ik_F n a} \Psi_L(na) + e^{ik_F n a} \Psi_R(na) \quad (5.30)$$

Some momentum cutoff of order $1/a$ is implied in the definition of the fields Ψ_L, Ψ_R , which represents no drawback since we are only interested in the low-energy properties of the model. Inserting (5.30) in the kinetic part of (5.29) we get, in the limit $a \rightarrow 0$,

$$\begin{aligned} -t \sum_{i,\sigma} \left(a_{i,\sigma}^+ a_{i+1,\sigma} + \text{h. c.} \right) \rightarrow \\ -iv_F \frac{1}{a} \int dx \left(-\Psi_{L\sigma}^+(x) \partial_x \Psi_{L\sigma}(x) + \Psi_{R\sigma}^+(x) \partial_x \Psi_{R\sigma}(x) \right) \quad (5.31) \\ v_F \equiv 2ta \sin(k_F a) \end{aligned}$$

The dimensions of the fermion fields are obtained simply by scaling them according to the lattice spacing a

$$a^{-1/2}\Psi_{L,R} \rightarrow \Psi_{L,R} \quad (5.32)$$

With regard to the interaction term in (5.29), the proposal is to promote the on-site interaction in the lattice to a delta-function type of interaction between density fields in continuous space[5]. The density operators built up from (5.30) have a divergent limit $a \rightarrow 0$, though, as a consequence of the infinite Fermi sea which appears in the continuum limit. We may regularize the product of Fermi fields by the normal order prescription, so that

$$\begin{aligned} a_{n\sigma}^+ a_{n\sigma} &\rightarrow : \Psi_{L\sigma}^+(x) \Psi_{L\sigma}(x) : + : \Psi_{R\sigma}^+(x) \Psi_{R\sigma}(x) : \\ &+ \left(e^{i2k_F x} \Psi_{L\sigma}^+(x) \Psi_{R\sigma}(x) + \text{h. c.} \right) \end{aligned} \quad (5.33)$$

The computation of $: \Psi_{L\sigma}^+ \Psi_{L\sigma} :$ and $: \Psi_{R\sigma}^+ \Psi_{R\sigma} :$ is now a little bit different in the discrete regularization of the theory, compared to the field theory approach of Chap. 4. The sensible bosonization formulas for the chiral fermion fields read (we omit spin indices for the time being)

$$\Psi_L(x) = \frac{1}{\sqrt{a}} e^{-i\Phi_L(x)} \quad (5.34)$$

$$\Psi_R(x) = \frac{1}{\sqrt{a}} e^{i\Phi_R(x)} \quad (5.35)$$

where we do not apply the boson normal order prescription but assume that the chiral boson fields have a momentum cutoff of order $1/\epsilon \equiv 2\pi/a$, i.e.

$$\Phi_R(x) = i \int_0^\infty \frac{dk}{\sqrt{k}} e^{-\epsilon k/2} \left(e^{-ikx} B_k^+ - e^{ikx} B_k \right) \quad (5.36)$$

$$\Phi_L(x) = i \int_{-\infty}^0 \frac{dk}{\sqrt{|k|}} e^{-\epsilon|k|/2} \left(e^{-ikx} B_k^+ - e^{ikx} B_k \right) \quad (5.37)$$

With this regularization the calculation of an electron correlator can be done following similar steps as in (5.17). For free boson fields we have, for instance,

$$\begin{aligned} \frac{1}{2\pi\epsilon} \langle e^{i\Phi_R(x)} e^{-i\Phi_R(y)} \rangle &= \frac{1}{2\pi\epsilon} \exp \left(- \int_0^\infty \frac{dp}{p} e^{-\epsilon p} \left(1 - e^{ip(x-y)} \right) \right) \\ &= \frac{1}{2\pi} \frac{i}{x-y+i\epsilon} \end{aligned} \quad (5.38)$$

which gives the free electron Green function with the correct causal prescription. By using the same method and a point-splitting technique[5], one may also check that

$$\Psi_L^+(x) \Psi_L(x) = \frac{1}{2\pi\epsilon} + \frac{1}{2\pi} \partial_x \Phi_L(x) \quad (5.39)$$

$$\Psi_R^+(x) \Psi_R(x) = \frac{1}{2\pi\epsilon} + \frac{1}{2\pi} \partial_x \Phi_R(x) \quad (5.40)$$

Normal ordering with reference to the Fermi level just gets rid of the divergent contributions in the limit $\epsilon \rightarrow 0$.

In terms of the chiral boson fields, the Hubbard hamiltonian becomes in the limit $a \rightarrow 0$

$$\begin{aligned}
H = & \frac{v_F}{4\pi} \int dx \left(: \partial_x \Phi_{L\uparrow} \partial_x \Phi_{L\uparrow} : + : \partial_x \Phi_{R\uparrow} \partial_x \Phi_{R\uparrow} : + \uparrow \leftrightarrow \downarrow \right) \\
& + Ua \int dx \left(\frac{1}{4\pi^2} (\partial_x \Phi_{L\uparrow} + \partial_x \Phi_{R\uparrow}) (\partial_x \Phi_{L\downarrow} + \partial_x \Phi_{R\downarrow}) \right. \\
& \left. + (\Psi_{L\uparrow}^+ \Psi_{R\uparrow} \Psi_{R\downarrow}^+ \Psi_{L\downarrow} + \text{h. c.}) \right) \quad (5.41)
\end{aligned}$$

In spite of its appearance, the interaction entering in (5.41) has a sensible limit $a \rightarrow 0$. We recall that its effective strength is given by $\sim Ua/v_F$, which is a finite quantity in the continuum limit as long as k_F is appropriately scaled with a . What is not so evident is the scaling of the backscattering term in the last line of (5.41) and, therefore, if the model may fall into the Luttinger liquid universality class. We may still give a complete transcription of the hamiltonian in terms of boson fields, using formulas (5.34) and (5.35),

$$\begin{aligned}
H = & \frac{v_F}{2} \int dx \left(4\pi \Pi_{\uparrow}^2(x) + \frac{1}{4\pi} (\partial_x \Phi_{\uparrow}(x))^2 + \uparrow \leftrightarrow \downarrow \right) \\
& + Ua \int dx \left(\frac{1}{4\pi^2} (\partial_x \Phi_{\uparrow}(x)) (\partial_x \Phi_{\downarrow}(x)) \right. \\
& \left. + \frac{1}{(2\pi\epsilon)^2} (e^{i\Phi_{\uparrow}(x)} e^{-i\Phi_{\downarrow}(x)} + e^{i\Phi_{\downarrow}(x)} e^{-i\Phi_{\uparrow}(x)}) \right) \quad (5.42)
\end{aligned}$$

with

$$\Phi_{\sigma}(x) = \Phi_{L\sigma}(x) + \Phi_{R\sigma}(x) \quad (5.43)$$

Introducing charge and spin fields

$$\Phi_c = \frac{1}{\sqrt{2}}(\Phi_{\uparrow} + \Phi_{\downarrow}) \quad , \quad \Phi_s = \frac{1}{\sqrt{2}}(\Phi_{\uparrow} - \Phi_{\downarrow}) \quad (5.44)$$

we see that the dynamics of these two kind of variables completely decouples in (5.42). The hamiltonian takes the form

$$\begin{aligned}
H = & \frac{v_F}{2} \int dx \left(4\pi \Pi_c^2(x) + \frac{1}{4\pi} (\partial_x \Phi_c(x))^2 \right) \\
& + Ua \frac{1}{8\pi^2} \int dx (\partial_x \Phi_c(x))^2 \\
& + \frac{v_F}{2} \int dx \left(4\pi \Pi_s^2(x) + \frac{1}{4\pi} (\partial_x \Phi_s(x))^2 \right) \\
& - Ua \frac{1}{8\pi^2} \int dx (\partial_x \Phi_s(x))^2 \\
& + Ua \frac{2}{(2\pi\epsilon)^2} \int dx \cos(\sqrt{2}\Phi_s(x)) \quad (5.45)
\end{aligned}$$

The charge sector has the same boson expression as that of the Luttinger model, while the backscattering term gives rise to an interaction of the sine-Gordon

type in the spin sector. Following the same procedure as in (5.7), we bring the hamiltonian to a form easy to diagonalize, in the case that the sine-Gordon interaction were switched off,

$$\begin{aligned}
H &= \frac{v_c}{2} \int dx \left(4\pi\mu\Pi_c^2(x) + \frac{1}{4\pi\mu}(\partial_x\Phi_c(x))^2 \right) \\
&+ \frac{v_s}{2} \int dx \left(4\pi\eta\Pi_s^2(x) + \frac{1}{4\pi\eta}(\partial_x\Phi_s(x))^2 \right) \\
&+ Ua \frac{2}{(2\pi\epsilon)^2} \int dx \cos(\sqrt{2}\Phi_s(x))
\end{aligned} \tag{5.46}$$

where

$$v_c = v_F \sqrt{1 + Ua/(\pi v_F)} \quad v_s = v_F \sqrt{1 - Ua/(\pi v_F)} \tag{5.47}$$

$$\mu = \frac{1}{\sqrt{1 + Ua/(\pi v_F)}} \quad \eta = \frac{1}{\sqrt{1 - Ua/(\pi v_F)}} \tag{5.48}$$

The charge dynamics can be mapped to a free field theory by a canonical transformation of the same type as (5.9). A similar transformation in the spin sector

$$\begin{aligned}
\Phi_s(x) &= \sqrt{\eta}\tilde{\Phi}_s(x) \\
\Pi_s(x) &= \frac{1}{\sqrt{\eta}}\tilde{\Pi}_s(x)
\end{aligned} \tag{5.49}$$

leads to a hamiltonian H_s for the spin variables

$$\begin{aligned}
H_s &= \frac{v_s}{2} \int dx \left(4\pi\tilde{\Pi}_s^2(x) + \frac{1}{4\pi}(\partial_x\tilde{\Phi}_s(x))^2 \right) \\
&+ Ua \frac{2}{(2\pi\epsilon)^2} \int dx \cos(\sqrt{2\eta}\tilde{\Phi}_s(x))
\end{aligned} \tag{5.50}$$

In order to ascertain if the spin dynamics corresponds to that of a Luttinger liquid (and, in particular, if it is gapless) one has to check the relevance or irrelevance of the last term in (5.50). This can be done by looking at the scaling dimension of this operator as $\epsilon \rightarrow 0$. We recall once again that the effective coupling constant is given by $\sim Ua/v_F$, so that when taking the limit we do not mind about the factor Ua in front of the interaction term. The scaling dimension can be extracted from the correlator of the cosine operator[5], as we did at the end of the previous section. We get

$$\begin{aligned}
\frac{1}{\epsilon^4} \langle \cos(\sqrt{2\eta}\tilde{\Phi}_s(x)) \cos(\sqrt{2\eta}\tilde{\Phi}_s(y)) \rangle &\sim \frac{1}{\epsilon^4} \langle e^{i\sqrt{2\eta}\tilde{\Phi}_s(x)} e^{-i\sqrt{2\eta}\tilde{\Phi}_s(y)} \rangle \\
&\sim \frac{1}{\epsilon^4} \left(\frac{\epsilon^2}{(x-y)^2} \right)^{2\eta}
\end{aligned} \tag{5.51}$$

For the case of repulsive interaction that we are treating here, it is clear that $\eta > 1$, so that the sine-Gordon interaction scales to zero in the continuum limit $\epsilon \rightarrow 0$.

Thus, we may conclude that the Hubbard model at weak coupling is a system with a gapless spectrum of charge and spin excitations. In the above considerations it is also implicit that the states of the system can be divided in two disjoint sectors of charge and spin, respectively, at least in the low-energy region of the spectrum. Unfortunately, it is also clear from the above treatment that the applicability of our continuum approach has a limit at a point in which U/t is $\sim O(1)$, where formulas like (5.47) and (5.48) become meaningless. It seems therefore that a sufficiently large on-site repulsion in the lattice becomes too rough to admit a smooth description in terms of our field variables and that the inability to capture strong correlation effects in the model is signaled by the shortcoming of our continuum theory. The singularity in equations (5.47) and (5.48) cannot have any physical meaning in any event, as long as the exact solution of the model does not show any discontinuity for $U \neq 0$.

5.3.2 Large- U Limit. Correlation Functions

We investigate at this point the other extreme situation in the Hubbard model, namely that in which the on-site repulsion U is sent to infinity. The interest in considering this limit is that in such case the Bethe ansatz equations simplify considerably and more information is then available from them. We are not going into the analysis of the equations since we can easily take the main conclusions of their study. To begin with, the first important fact is that, in the limit $U \rightarrow \infty$, the ground state wavefunction of the system splits into a factor for the charge variables times another factor for the spin variables[10]. That is, the separation of charge and spin is an exact property of the Hubbard model in the limit $U \rightarrow \infty$. Moreover, the wavefunction of the spin variables corresponds to that of a spin-1/2 antiferromagnetic Heisenberg chain, getting rid of the holes in the system. The isotropic antiferromagnet belongs to the Luttinger liquid universality class and its low-energy properties are given by a Luttinger model hamiltonian

$$H_s = \frac{v_s}{2} \int dx \left(4\pi \Pi_s^2(x) + \frac{1}{4\pi} (\partial_x \Phi_s(x))^2 \right) \quad (5.52)$$

The dynamics of the charge sector is more subtle. In the limit of very large on-site repulsion, it becomes very unfavorable for the system to have two fermions on the same site, so that it mainly remains in a configuration in which each particle is confined between its nearest neighbors. These strong correlation effects are of the kind we have already seen in the harmonic chain. Therefore, we may tentatively introduce the hypothesis that the charge dynamics is governed by a hamiltonian like (5.7)

$$H_c = \frac{v_c}{2} \int dx \left(4\pi \mu \Pi_c^2(x) + \frac{1}{4\pi \mu} (\partial_x \Phi_c(x))^2 \right) \quad (5.53)$$

In the above expression v_c and μ are parameters to be determined. They can be fixed from the information that one can extract in the Bethe ansatz resolution of the model. In particular, v_c can be obtained from the spectrum of the low-energy

charge excitations. The value of μ can be determined from the compressibility of the system. We recall that the constant mode in $\sqrt{2}\partial_x\Phi_c/(2\pi)$ is to be identified with the particle density n in the model. Therefore, taking the derivative of (5.53) with respect to n and applying the Hellman-Feynman theorem we get[6]

$$\frac{1}{L} \frac{\partial^2 E_0}{\partial n^2} = \frac{\pi v_c}{2 \mu} \quad (5.54)$$

where E_0 is the ground state energy of the system. The left-hand-side of (5.54) is nothing but the inverse of the compressibility and can be obtained numerically from Lieb and Wu exact solution. Nice curves of μ as a function of the on-site repulsion U and the particle density n obtained by this method are shown in Ref. [6]. From them one gets clear evidence that in the limit of very large repulsion $\mu \rightarrow 1/2$, irrespective of the value of the particle density.

The knowledge of the μ parameter is of particular interest, since it dictates the long-distance behavior of a number of correlators. The general structure of the correlation functions of the discrete model is, at large x ,

$$\langle \Psi(x)\Psi^+(0) \rangle = a_0 \frac{1}{x^{\alpha_0}} \cos(k_F x) + a_1 \frac{1}{x^{\alpha_1}} \cos(3k_F x) + \dots \quad (5.55)$$

$$\langle \rho(x)\rho(0) \rangle = \frac{\mu}{\pi^2} \frac{1}{x^2} + b_1 \frac{1}{x^{\beta_1}} \cos(2k_F x) + b_2 \frac{1}{x^{\beta_2}} \cos(4k_F x) + \dots \quad (5.56)$$

$$\langle \sigma(x)\sigma(0) \rangle = \frac{1}{\pi^2} \frac{1}{x^2} + c_1 \frac{1}{x^{\gamma_1}} \cos(2k_F x) + \dots \quad (5.57)$$

$\rho(x)$ being the charge density operator and $\sigma(x)$ the spin density operator. We are omitting at this point logarithmic corrections to the above power-law decays, which affect in particular to the $2k_F$ harmonic contributions to the charge density and spin density correlators[11]. The $4k_F$ and higher harmonics in these functions, as well as the $3k_F$ and higher harmonics in the electron Green function, arise due to the discrete character of the model[12], as we already learned from the study of the harmonic chain. These contributions cannot be obtained sticking strictly to the computational framework of the Luttinger model and their consideration requires a modification of the standard bosonization formulas incorporating the lattice effects[13].

The critical exponents giving the dominant behavior in equations (5.55)-(5.57) have been estimated numerically in the large- U limit by several authors. We are now in a position to test whether the Luttinger model description synthesized by (5.52) and (5.53) is able to predict the correct values of the exponents. Focusing first on the electron Green function, the determination of α_0 follows the same steps as in (4.71). We have to remind the correspondence (5.11) between μ and $\cosh \phi$ in that equation, which gives in the present case $c^2 = 9/8$. Thus, we are predicting an exponent $\alpha_0 = 9/8$ for the dominant behavior of the electron Green function. In a numerical computation one usually measures some observable defined from that object as, for instance, the momentum distribution function. In our Luttinger model description, this must have a singular behavior at k_F of the type (4.77), with $s^2 = 1/8$. The numerical estimates range

between 0.13 and 0.15 [10], and a refined finite size analysis of the results gives an exponent ≈ 0.126 [14]. This is in very good agreement with the theoretical prediction, taking into account that the extrapolations are made from measures over relatively small systems.

Regarding the charge density and spin density correlators, the $1/x^2$ contributions stem from the correlations of the first two terms in (5.33), while the $2k_F$ oscillations arise from the hybridization of left and right modes in the density fields. In the case of the charge density, for instance, we have

$$\rho(x) = \frac{\sqrt{2}}{2\pi} \partial_x \Phi_c + \frac{1}{2\pi\epsilon} \left(e^{i2k_F x} e^{i\Phi_\uparrow} + \text{h. c.} \right) + \frac{1}{2\pi\epsilon} \left(e^{i2k_F x} e^{i\Phi_\downarrow} + \text{h. c.} \right) \quad (5.58)$$

We need to compute the correlators between the $2k_F$ harmonics in (5.58). This can be done again making first the transformation to free fields and using the formula (5.18). We have, for instance,

$$\begin{aligned} \langle e^{i\Phi_\uparrow(x)} e^{-i\Phi_\uparrow(0)} \rangle &= \\ &= \langle e^{i\sqrt{\mu}\tilde{\Phi}_c(x)/\sqrt{2}} e^{i\Phi_s(x)/\sqrt{2}} e^{-i\sqrt{\mu}\tilde{\Phi}_c(0)/\sqrt{2}} e^{-i\Phi_s(0)/\sqrt{2}} \rangle \\ &\sim \frac{1}{(x^2)^{\mu/2}} \frac{1}{(x^2)^{1/2}} = \frac{1}{|x|^{\mu+1}} \end{aligned} \quad (5.59)$$

It can be seen that our continuum approach gives the same prediction for the exponents β_1 in (5.56) and γ_1 in (5.57), which according to (5.59) is $\beta_1 = \gamma_1 = 3/2$. On the other hand, the spin correlation function has been the object of a thorough numerical investigation [10, 14]. The results of Ref. [10] place the exponent γ_1 between 1.3 and 1.45, while the finite size analysis of the same data seems to give $\gamma_1 \approx 1.48$ [14]. Again, this is a clear confirmation of the applicability of the Luttinger model description to the Hubbard model at very large on-site repulsion.

It has to be stressed that, contrary to the procedure followed in the weak coupling regime, we have not been able to formulate an analytical correspondence from the microscopic Hubbard hamiltonian in the large- U limit to the continuum field theory description of the model. In this sense, our approach has been rather heuristic. There have been also other attempts to develop a picture of the low-energy excitations of the model, at arbitrary U , either classifying the different states which appear in finite systems [15] or establishing the correspondence with conformal field theory through finite size scaling [8, 9]. The conclusion that one reaches is that the low-energy limit of the model may be given by a simple field theory (two $c = 1$ conformal field theories, one of them with varying radius of compactification), yet it is not known how to bring explicitly the strongly correlated system into the framework of continuum field theory.

References

- [1] See, for instance, V. J. Emery, *The Many-Body Problem in One Dimension*, in *Correlated Electron Systems*, Vol. 9, ed. V. J. Emery (World Scientific, Singapore, 1993).
- [2] S. Coleman, *Phys. Rev. D* **11** (1975) 2088.
- [3] For a review, see H. J. Schulz, *The Metal-Insulator Transition in One Dimension*, Lectures given at Los Alamos Meeting on Strongly Correlated Electron Systems, December 1993, database report cond-mat/9412036.
- [4] E. H. Lieb and F. Y. Wu, *Phys. Rev. Lett.* **20** (1968) 1445.
- [5] R. Shankar, *Bosonization: How to Make It Work for You in Condensed Matter*, Lectures given at the BCSPIN School, Katmandu, May 1991.
- [6] H. J. Schulz, *Phys. Rev. Lett.* **64** (1990) 2831.
- [7] P. W. Anderson and Y. Ren, *The One-Dimensional Hubbard Model with Repulsive Interaction* (unpublished).
- [8] N. Kawakami and S.-K. Yang, *Phys. Lett. A* **148** (1990) 359.
- [9] H. Frahm and V. E. Korepin, *Phys. Rev. B* **42** (1990) 10553.
- [10] M. Ogata and H. Shiba, *Phys. Rev. B* **41** (1990) 2326.
- [11] T. Giamarchi and H. J. Schulz, *Phys. Rev. B* **39** (1989) 4620.
- [12] F. D. M. Haldane, *Phys. Rev. Lett.* **47** (1981) 1840.
- [13] J. Ferrer, J. González and M.-A. Martín-Delgado, *Phys. Rev. B* **51** (1995) 4807.
- [14] S. Sorella, A. Parola, M. Parrinello and E. Tosatti, *Europhys. Lett.* **12** (1990) 721.
- [15] H. J. Schulz, *Interacting Fermions in One Dimension: From Weak to Strong Correlation*, in *Correlated Electron Systems*, Vol. 9, ed. V. J. Emery (World Scientific, Singapore, 1993).